Optimal Path and Minimal Spanning Trees in Random Weighted Networks

Contents

References   71

Optimal Path and Minimal Spanning Trees in Random Weighted Networks

Lidia A. Braunstein,[1,2] Zhenhua Wu,[2] Yiping Chen,[2] Sergey V. Buldyrev,[2,3] Tomer Kalisky,[4] Sameet Sreenivasan,[2] Reuven Cohen,[5,4] Eduardo López,[2,6] Shlomo Havlin,[4,2] and H. Eugene Stanley[2]

[1]*Departamento de Física, Facultad de Ciencias Exactas y Naturales,*
Universidad Nacional de Mar del Plata,
Funes 3350, 7600 Mar del Plata, Argentina[*]
[2]*Center for Polymer Studies, Boston University,*
Boston, Massachusetts 02215, USA
[3]*Department of Physics Yeshiva University,*
500 West 185th Street Room 1112,NY, 10033, USA
[4]*Minerva Center and Department of Physics,*
Bar-Ilan University, 52900 Ramat-Gan, Israel
[5] *Dept. of Electrical and Computer Engineering,*
Boston University, Boston, Massachusetts 02215, USA
[6]*Theoretical Division, Los Alamos National Laboratory,*
Mail Stop B258, Los Alamos, NM 87545 USA

3

Abstract

We review results on the scaling of the optimal path length ℓ_{opt} in random networks with weighted links or nodes. We refer to such networks as "weighted" or "disordered" networks. The optimal path is the path with minimum sum of the weights. In strong disorder, where the maximal weight along the path dominates the sum, we find that ℓ_{opt} increases dramatically compared to the known small world result for the minimum distance $\ell_{\mathrm{min}} \sim \log N$, where N is the number of nodes. For Erdős-Rényi (ER) networks $\ell_{\mathrm{opt}} \sim N^{1/3}$, while for scale free (SF) networks, with degree distribution $P(k) \sim k^{-\lambda}$, we find that ℓ_{opt} scales as $N^{(\lambda-3)/(\lambda-1)}$ for $3 < \lambda < 4$ and as $N^{1/3}$ for $\lambda \geq 4$. Thus, for these networks, the small-world nature is destroyed. For $2 < \lambda < 3$ in contrary, our numerical results suggest that ℓ_{opt} scales as $\ln^{\lambda-1} N$, representing still a small world. We also find numerically that for weak disorder $\ell_{\mathrm{opt}} \sim \ln N$ for ER models as well as for SF networks. We also review the transition between the strong and weak disorder regimes in the scaling properties of ℓ_{opt} for ER and SF networks and for a general distribution of weights τ, $P(\tau)$. For a weight distribution of the form $P(\tau) = 1/(a\tau)$ with $(\tau_{\mathrm{min}} < \tau < \tau_{\mathrm{max}})$ and $a = \ln \tau_{\mathrm{max}}/\tau_{\mathrm{min}}$, we find that there is a crossover network size $N^* = N^*(a)$ at which the transition occurs. For $N \ll N^*$ the scaling behavior of ℓ_{opt} is in the strong disorder regime, while for $N \gg N^*$ the scaling behavior is in the weak disorder regime. The value of N^* can be determined from the expression $\ell_\infty(N^*) = ap_c$, where ℓ_∞ is the optimal path length in the limit of strong disorder, $A \equiv ap_c \to \infty$ and p_c is the percolation threshold of the network. We suggest that for any $P(\tau)$ the distribution of optimal path lengths has a universal form which is controlled by the scaling parameter $Z = \ell_\infty/A$ where $A \equiv p_c\tau_c / \int_0^{\tau_c} \tau P(\tau)d\tau$ plays the role of the disorder strength and τ_c is defined by $\int_0^{\tau_c} P(\tau)d\tau = p_c$. In case $P(\tau) \sim 1/(a\tau)$, the equation for A is reduced to $A = ap_c$. The relation for A is derived analytically and supported by numerical simulations for Erdős-Rényi and scale-free graphs. We also determine which form of $P(\tau)$ can lead to strong disorder $A \to \infty$. We then study the minimum spanning tree (MST), which is the subset of links of the network connecting all nodes of the network such that it minimizes the sum of their weights. We show that the minimum spanning tree (MST) in the strong disorder limit is composed of percolation clusters, which we regard as "super-nodes", interconnected by a scale-free tree. The MST is also considered to be the skeleton of the network where the main transport occurs. We furthermore show that the MST can be partitioned into two distinct components, having significantly different transport properties, characterized by centrality — number of times a node (or link) is used by transport paths. One component the *superhighways*,

for which the nodes (or links) with high centrality dominate, corresponds to the largest cluster at the percolation threshold (incipient infinite percolation cluster) which is a subset of the MST. The other component, *roads*, includes the remaining nodes, low centrality nodes dominate. We find also that the distribution of the centrality for the incipient infinite percolation cluster satisfies a power law, with an exponent smaller than that for the entire MST. We demonstrate the significance identifying the superhighways by showing that one can improve significantly the global transport by improving a very small fraction of the network, the superhighways.

---

*Electronic address: lbrauns@mdp.edu.ar

I.   INTRODUCTION

Recently much attention has been focused on the topic of complex networks which characterize many biological, social, and communication systems [Albert & Barabási, 2002; Mendes *et al.*, 2003; Pastor-Satorras & Vespignani, 2004]. The networks are represented by nodes associated to individuals, organizations, or computers and by links representing their interactions. The classical model for random networks is the Erdős-Rényi (ER) model [Erdős & Rényi, 1959; Erdős & Rényi, 1960; Bollobas, 1985]. An important quantity characterizing networks is the average distance (minimal hopping) $\ell_{\min}$ between two nodes in the network of total N nodes. For the Erdős-Rényi network $\ell_{\min}$ scales as $\ln N$ [Bollobas, 1985], which leads to the concept of "small worlds" or "six degrees of separation". For scale-free (SF) [Albert & Barabási, 2002] networks $\ell_{\min}$ scales as $\ln \ln N$, this leads to the concept of ultra small worlds [Cohen *et al.*, 2002; Mendes *et al.*, 2003].

In most studies, all links in the network are regarded as identical and thus a crucial parameter for information flow including efficient routing, searching, and transport is $\ell_{\min}$. In practice, however, the weights (e.g., the quality or cost) of links are usually not equal [Barrat *et al.*, 2004; Boccaletti *et al.*, 2006].

Thus the length of the optimal path ℓ_{opt}, minimizing the sum of weights, is usually longer than $\ell_{\min}$. For example, the cost could be the time required to transit the link. There are often many traffic routes from site A to site B with a set of transit time τ_i, associated with each link along the path. The fastest (optimal) path is the one for which $\sum_i \tau_i$ is a minimum, and often the optimal path has more links than the shortest path. In many cases, the selection of the path is controlled by most of the weights (e.g., total cost) contributing to the sum. This case corresponds to weak disorder (WD). However, in other cases, for example when the distribution of disorder is very broad a *single* weight dominates the sum. This situation—in which one link controls the selection of the path—is called the strong disorder limit (SD).

For a recent quantitative criterion for SD and WD, see Ref. [Chen *et. al*, 2006] and Section VI(B) in this article.

The strong disorder is relevant *e.g.* for computer and traffic networks, since the slowest link in communication networks determines the connection speed. An example for SD is when a transmission at a constant high rate is needed (e.g., in broadcasting video records

over the Internet). In this case the narrowest band link in the path between the transmitter and receiver controls the rate of transmission. This limit is also called the "ultrametric" limit and we refer to the optimal path in this limit as the min-max path.

The SD limit is also related to the minimal spanning tree which includes all optimal paths between all pairs of sites in the network. The disorder on a network is usually implemented from a distribution $P(\tau) \sim 1/(a\tau)$, where $1 < \tau < e^a$ [Porto *et al.*, 1999; Braunstein *et al.*, 2001; Cieplak *et al.*, 1996; Braunstein *et al.*, 2003]. We assign to each link of the network a random number r, uniformly distributed between 0 and 1. The cost associated with link i is then $\tau_i \equiv \exp(ar_i)$ where a is the parameter which controls the broadness of the distribution of link costs. The parameter a represents the strength of disorder. The limit $a \to \infty$ is the strong disorder limit, since for this case clearly only one link dominates the cost of the path. The strong disorder limit (SD) can be implemented in a disordered media by assigning to each link a potential barrier ϵ_i so that τ_i is the time to cross this barrier in a thermal activation process. Thus $\tau_i = e^{\epsilon_i/KT}$, where K is the Boltzmann constant and T is absolute temperature. The optimal path corresponds to the minimum $(\sum_i \tau_i)$ over all possible paths. We can define disorder strength $a = 1/KT$. When $a \to \infty$, only the largest τ_i dominates the sum. Thus, $T \to 0$ (very low temperature) corresponds to the strong disorder limit.

There are distinct scaling relationships between the length of the average optimal path ℓ_{opt} and the network size (number of nodes) N depending on whether the network is strongly or weakly disordered [Porto *et al.*, 1999, Braunstein *et al.*, 2003]. It was shown using percolation arguments (See Section IV) that for strong disorder [Braunstein *et al.*, 2003], $\ell_{opt} \sim N^{\nu_{opt}}$, where $\nu_{opt} = 1/3$ for Erdős-Rényi (ER) random networks [Erdős & Rényi, 1959] and for scale-free (SF) [Albert & Barabási, 2002] networks with $\lambda > 4$, where λ is the exponent characterizing the power law decay of the degree distribution. For SF networks with $3 < \lambda < 4$, $\nu_{opt} = (\lambda - 3)/(\lambda - 1)$. For $2 < \lambda < 3$, percolation arguments do not work, but the numerical results suggest $\ell_{opt} \sim \ln^{\lambda-1} N$, which is again much larger than the ultra small result for the shortest path $\ell_{min} \sim \ln \ln N$ found for $2 < \lambda < 3$ in Ref. [Cohen & Havlin, 2003]. When the weights are taken from a uniform distribution we are in the weak disorder limit. In this case $\ell_{opt} \sim \ln N$ for both ER and SF for all the values of λ [Braunstein *et al.*, 2003]. For $2 < \lambda < 3$, this result is significantly different from the ultra small world result found for unweighed networks.

Porto [Porto *et al.*, 1999] considered the optimal path transition from weak to strong

disorder for 2-D and 3-D lattices, and found a crossover in the scaling properties of the optimal path that depends on the disorder strength a, as well as the lattice size L (see also [Buldyrev *et al.*, 2006]). Similar to regular lattices, there exists for any finite a, a crossover network size $N^*(a)$ such that for $N \ll N^*(a)$, the scaling properties of the optimal path are in the strong disorder regime while for $N \gg N^*(a)$, the network is in the weak disorder regime. The function $N^*(a)$ was evaluated. Moreover, a general criterion to determine which form of $P(\tau)$ can lead to strong disorder, and a general condition when strong or weak disorder occurs was found analytically [Chen *et. al*, 2006]. The derivation was supported by extensive simulations.

The study of the distribution of the length of the optimal paths in a network was reported in Ref. [Kalisky *et al.*, 2005]. It was found that the distribution has the scaling form $P(\ell_{\rm opt}, N, a) \sim \frac{1}{\ell_\infty} G\left(\frac{\ell_{\rm opt}}{\ell_\infty}, \frac{1}{p_c}\frac{\ell_\infty}{a}\right)$, where ℓ_∞ is $\ell_{\rm opt}$ for $a \to \infty$ and p_c is the percolation threshold. It was also shown that a single parameter $Z \equiv \frac{1}{p_c}\frac{\ell_\infty}{a}$ determines the functional form of the distribution. Importantly, it was found [Chen *et. al*, 2006] that for all $P(\tau)$ that possess a strong-weak disorder crossover, the distributions $P(\ell_{\rm opt})$ of the optimal path lengths display the same universal behavior.

Another interesting question is about a possible origin of scale-free degree distribution with $\lambda = 2.5$ in some real world networks. Kalisky [Kalisky *et. al*, 2006] introduced a simple process that generates random scale-free networks with $\lambda = 2.5$ from weighted Erdös-Rényi graphs [Erdős & Rényi, 1960]. They found that the minimum spanning tree (MST) on an Erdös-Rényi graph is composed of percolation clusters, which we regard as "super nodes", interconnected by a scale-free tree with $\lambda = 2.5$.

Known as the tree with the minimum weight among all possible spanning tree, the MST is also the union of all "strong disorder" optimal paths between any two nodes [Barabási, 1996; Dobrin & Duxbury, 2001; Cieplak *et al.*, 1996; Porto *et al.*, 1999; Braunstein *et al.*, 2003; Wu *et al.*, 2005]. As the global optimal tree, the MST plays a major role for transport process, which is widely used in different fields, such as the design and operation of communication networks, the travelling salesman problem, the protein interaction problem, optimal traffic flow, and economic networks [Khan *et al.*, 2003; Skiena, 1990; Fredman & Tarjan, 1987; Kruskal, 1956; Macdonald *et. al*, 2005; Bonanno *et al.*, 2003; Onnela *et al.*, 2003]. One important question in network transport is how to identify the nodes or links that are more important than others. A relevant quantity that characterizes transport in networks is the

betweenness centrality, C, which is the number of times a node (or link) used by all optimal paths between all pairs of nodes [Newman, 2001; Goh *et al.*, 2001; Kim *et al.*, 2004]. For simplicity we call the "betweenness centrality" here "centrality" and we use the notation "nodes" but similar results have been obtained for links. The centrality, C, quantifies the "importance" of a node for transport in the network. Moreover, identifying the nodes with high C enables us to improve their transport capacity and thus improve the global transport in the network. The probability density function (pdf) of C was studied on the MST for both SF [Barabási & Albert, 1999] and ER [Erdős & Rényi, 1959; Erdős & Rényi, 1960] networks and found to satisfy a power law, $\mathcal{P}_{\mathrm{MST}}(C) \sim C^{-\delta_{\mathrm{MST}}}$, with δ_{MST} close to 2 [Goh *et al.*, 2005; Kim *et al.*, 2004]. However, Ref. [Wu *et al.*, 2006] found that a sub-network of the MST,[1] the infinite incipient percolation cluster (IIC) has a significantly higher average C than the entire MST — i.e., the set of nodes inside the IIC are typically used by transport paths more often than other nodes in the MST (See Section IX). In this sense the IIC can be viewed as a set of *superhighways* (SHW) in the MST. The nodes on the MST which are not in the IIC are called *roads*, due to their analogy with roads which are not superhighways (usually used by local residents). Wu *et al.* [Wu *et al.*, 2006] demonstrate the impact of this finding by showing that improving the capacity of the superhighways (IIC) is significantly a better strategy to enhance global transport compared to improving the same number of links of the highest C in the MST, although they have higher C.[2] This counterintuitive result shows the advantage of identifying the IIC subsystem, which is very small and of oder zero compared to the full network.[3]

II. ALGORITHMS

A. Construction of the Networks

To construct an ER network of size N with average node degree $\langle k \rangle$, we start with $\langle k \rangle N/2$ edges and randomly pick a pair of nodes from the total possible $N(N-1)/2$ pairs to connect with an edge. The only condition we impose is that there cannot be multiple edges between two nodes. When $\langle k \rangle > 1$ almost all nodes of the network will be connected with high probability.

To generate scale-free (SF) graphs of size N, we employ the Molloy-Reed algorithm

[Molloy & Reed, 1998]. Initially the degree of each node is chosen according to a scale-free distribution, where each node is given a number of open links or "stubs" according to its degree. Then, stubs from all nodes of the network are interconnected randomly to each other with two constraints that there are no multiple edges between two nodes and that there are no looped edges with identical ends. The exact form of the degree distribution is usually taken to be

$$P(k) = ck^{-\lambda} \qquad k = m, \cdots K \tag{1}$$

where m and K are the minimal and maximal degrees, and $c \approx (\lambda-1)m^{\lambda-1}$ is a normalization constant . For real networks with finite size, the highest degree K depends on network size N: $K \approx mN^{1/(\lambda-1)}$, thus creating a "natural" cutoff for the highest possible degree . When $m > 1$ there is a high probability that the network is fully connected.

B.   Dijkstra's algorithm

The Dijkstra's algorithm [Cormen *et al.*, 1990] is used in general to find the optimal path, when the weights are drawn from an arbitrary distribution. The search for the optimal path follows a procedure akin to "burning" where the "fire" starts from our chosen origin. At the beginning, all nodes are given a distance ∞ except the origin which is given a distance 0. At each step we choose the next unburned node which is nearest to the origin, and "burn" it, while updating the optimal distance to all its neighbors. The optimal distance of a neighbor is updated only if reaching it from the current burning node gives a total path length that is shorter than its current distance.

C.   Ultrametric Optimization

Next we describe a numerical method for computing ℓ_{opt} between any two nodes in strong disorder [Dobrin & Duxbury, 2001; Braunstein *et al.*, 2001]. In this case the sum of the weights must be completely dominated by the largest weight. Sometimes this condition is referred as ultrametric. We can satisfy this condition assigning weights to all the links $\tau_i = \exp(ar_i)$ choosing a to be so large, that any two links will have different binary orders of magnitude. For example, if we can select $0 \leq r_i < 1$ from a uniform distribution, using a 48-bit random number generator, there will be no two identical values of r_i in a system of

any size that we study. In this case $\Delta r_i \geq 2^{-48}$ and we can select $a \geq 2^{48} \ln 2$ to guarantee the strong disorder limit. To find the optimal paths under the ultrametric condition, we start from one node (the origin—see Fig. 1) and visit all the other nodes connected to the origin using a burning algorithm. If a node at distance ℓ_0 (from the origin) is being visited for the first time, this node will be assigned a list S_0 of weights τ_{0i}, $i = 1 \cdots \ell_0$ of the links by which we reach that node sorted in descending order. Since $\tau_{0i} = exp(ar_{0i})$, we can use a list of random numbers r_{0i} instead.

$$S_0 = \{r_{01}, r_{02}, r_{03}, ...r_{0l_0}\}, \tag{2}$$

with $r_{0j} > r_{0j+1}$ for all j. If we reach a node for a second time by another path of length ℓ_1, we define for this path a new list S_1,

$$S_1 = \{r_{11}, r_{12}, r_{13}, \ldots r_{1l_1}\}, \tag{3}$$

and compare it with S_0 previously defined for this node.

Different sequences can have weights in common because some paths have links in common because of the loops, so it is not enough to identify the sequence by its maximum weight; in this case it must also be compared with the second maximum, the third maximum, etc. We define $S_p < S_q$ if there exists a value m, $1 \leq m \leq \min(\ell_p, \ell_q)$ such that

$$
\begin{aligned}
r_{pj} = r_{qj} \qquad &\text{for} \qquad 1 \leq j < m \qquad \text{and} \\
r_{pj} < r_{qj} \qquad &\text{for} \qquad j = m,
\end{aligned}
\tag{4}
$$

or if $\ell_q > \ell_p$ and $r_{pj} = r_{qj}$ for all $j \leq \ell_p$. If $S_1 < S_0$, we replace S_0 by S_1. The procedure continues until all paths have been explored and compared. At this point, $S_0 = S_{\text{opt}}$, where S_{opt} is the sequence of weights for the optimal path of length ℓ_{opt}. A schematic representation of this ultrametric algorithm is presented in Fig. 1. This algorithm is slow and memory consuming since we have to keep track of a sequence of values and the rank. Using this method, we obtain systems of sizes up to 2^{12} nodes, typically 10^5 realizations of disorder.

D. Bombing Optimization

This algorithm allows to compute ℓ_{opt} (and other relevant quantities) between any two nodes in strong disorder limit and was introduced by Cieplak *et al.* [Cieplak *et al.*, 1996].
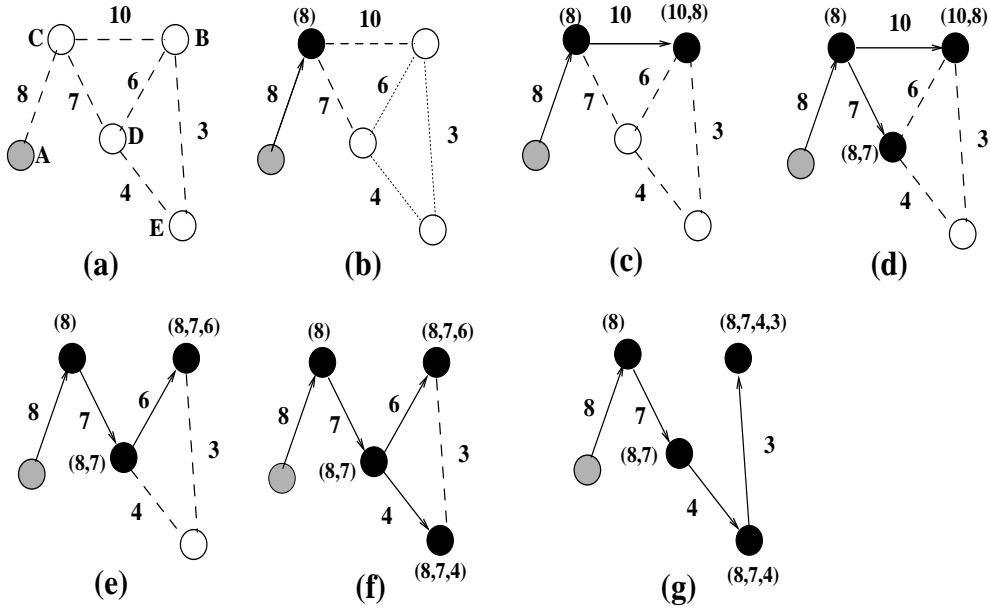
FIG. 1: In (a) we show schematically a network consisting of five nodes (A, B, C, D, and E). The links between them are shown in dashed lines. The origin (A) is marked in gray. All links were assigned random weights, shown beside the links. In (b) one node (C) has been visited for the first time (marked in black) and assigned the sequence (8) of length $\ell = 1$. The path is marked by a solid arrow. Notice that there is no other path going from the origin (A) to this node (C) so $\ell_{\text{opt}} = 1$ for that path. In (c) another node (B) is visited for the first time (marked in black) and assigned the sequence $(10, 8)$ of length 2. The sequence has the information of all the weights of that path arranged in decreasing order. In (d) another node (D) is visited for the first time and assigned the sequence $(8, 7)$ of length 2. In (e), node (B) visited in (c) with sequence $(10, 8)$ is visited again with sequence $(8, 7, 6)$. The last sequence is smaller than the previous sequence $(10, 8)$ so that node (B) is reassigned the sequence $(8, 7, 6)$ of length 3 [See Eq. (4)]. The new path is shown as a solid line. In (f) a new node (E) is assigned with sequence $(8, 7, 4)$. In (g) node (B) is reached for the third time and reassigned the sequence $(8, 7, 4, 3)$ of length 4. The optimal path for this configuration from A to B is denoted by the solid arrows in (g) (After [Havlin *et al.*, 2005]).

Basically the algorithm does the following

1. Sort the edges by descending weight.

2. If the removal of the highest weight edge will not disconnect A from B – remove it.

12

3. Go back to step 2 until all edges have been processed.

Since the edge weights are random, so is the ordering. Therefore, in fact, one does not need even to select edge weights and "bombing" algorithm can be simplified by removing randomly chosen edges one at a time, provided that their removal does not break the connectivity between the two nodes. The bottleneck of this algorithm is checking the connectivity after each removal. To speed it up, we first compute the minimal path between nodes A and B using Dijkstra's algorithm. Then we must check the connectivity only if the removed bond belongs to this path. In this case, we attempt to compute a new minimal path between A and B on the subset of remaining bonds. If our attempt fails, it means that the removal of this bond would destroy the connectivity between A and B. Therefore, we restore this bond and exclude it from the list of bonds subject to random removal. With this improvement we could reach systems of sizes up to 2^{16} nodes and 10^5 realizations of weight disorder.

E.   The Minimum Spanning Tree (MST)

The MST on a weighted graph is a tree that reaches all nodes of the graph and for which the sum of the weights of all the links or nodes (total weight) is minimal. Also, in the "strong disorder" limit, each path between two sites on the MST is the optimal path [Cieplak *et al.*, 1996; Dobrin & Duxbury, 2001], meaning that along this path the maximum *barrier* (weight) is the smallest possible [Dobrin & Duxbury, 2001; Braunstein *et al.*, 2003; Sreenivasan *et al.*, 2004]. Standard algorithms for finding the MST are Prim's algorithm [Cormen *et al.*, 1990] which resembles invasion percolation [Bunde & Havlin, 1996] and Kruskal's algorithm [Cormen *et al.*, 1990]. First we explain the Prim's algorithm.

(a) Create a tree containing a single vertex, chosen arbitrarily from the graph.

(b) Create a set containing all the edges in the graph.

(c) Remove from the set an edge with minimum weight that connects a vertex in the tree with a vertex not in the tree.

(d) Add that edge to the tree.

(e) Repeat steps (c-d) until every edge in the set connects two vertices in the tree.

13

Note that two nodes in the tree cannot be connected again by a link, thus forbidding loops to be formed. Prim's algorithm essentially starts by choosing a random node in the network, and then growing outward to the "cheapest" link which is adjacent to the starting node. Each link which is "invaded" is added to the growing cluster (tree), and the process is iterated until every site has been reached. Bonds can only be invaded if they do not produce a loop, so that the tree structure is maintained [20]. This process resembles invasion percolation with trapping studied in the physics literature [Barabási, 1996; Porto et al., 1997]. A direct consequence of the invasion process is that a path between two sites A and B on the MST is the path whose maximum weight is minimal, i.e., the minimal-barrier path. This is because if there were another path with a smaller barrier (i.e. maximal weight link) connecting A and B, the invasion process would have chosen that path to be on the MST instead. The minimal-barrier path is important in cases where the "bottleneck" link is important. For example, in streaming video broadcast on the Internet, it is important that each link along the path to the client will have enough capacity to support the transmission rate, and even one link with not enough bandwidth can become a bottleneck and block the transmission. In this case we will choose the minimal-barrier path rather than the optimal path. An equivalent algorithm for generating the MST is the Kruskal's algorithm:

(a) Create a forest F (a set of trees), where each vertex in the graph is a separate tree.

(b) Create a set S containing all the edges in the graph.

(c) While S is nonempty: " Remove an edge with minimum weight from S. " If that edge connects two different trees, then add it to the forest, combining two trees into a single tree. " Otherwise discard that edge. Note that an edge cannot connect a tree to itself, thus forbidding loops to be formed.

Kruskal's algorithm resembles the percolation process because we add links to the forest according to increasing order of weights. The forest is actually the set of percolation clusters growing as the occupation probability is increasing. It was noted by Dobrin et al. [Dobrin & Duxbury, 2001] that the geometry of the MST depends only on the unique ordering of the links of the network according to their weights. It does not matter if the weights are nearly the same or wildly different, it is only their ordering that matters. Given a network with weights on the links, any transformation which preserves the ordering of the weights (e.g.,

the link which has the fiftieth largest energy is the same before and after the transformation) leaves the MST geometry unaltered. This property is termed "universality" of the MST. Thus, given a network with weights, represented by a random variable distributed uniformly, a monotonic transformation of the weights will leave the MST unchanged.

Another equivalent algorithm to find the MST is the "bombing optimization algorithm" [Braunstein *et al.*, 2003]. Similar to the one explained in Section II D, we start with the full network and remove links in order of descending weights. If the removal of a link disconnects the graph, we restore the link [Ioselevich & Lyubshin, 2004]; otherwise the link is removed. The algorithm ends and the MST is obtained when no more links can be removed without disconnecting the graph.

F.   The Incipient Infinite Cluster (IIC)

To find the IIC of ER and SF in uncorrelated weighted networks,[4] we start with the fully connected network and remove links in descending order of their weights. After each removal of a link, we calculate the weighted average degree $\kappa \equiv \langle k^2 \rangle / \langle k \rangle$, which decreases with link removals. When $\kappa < 2$, we stop the process [Cohen *et al.*, 2000]. The meaning of this criterion is explained in the next section, where its connection with the percolation threshold p_c is established. The largest remaining component is the IIC. For the two dimensional (2D) square lattice we cut the links (bonds) in descending order of their weights until we reach the percolation threshold p_c (= 0.5). At that point the largest remaining component is the IIC [Bunde & Havlin, 1996].

III.   OPTIMAL PATH IN STRONG DISORDER AND PERCOLATION ON THE CAYLEY TREE.

In this section we review classical analytical methods for exploring random networks based on percolation theory on a Cayley tree [Stauffer & Aharony, 1994; Bunde & Havlin, 1996], or branching processes [Harris, 1989]. To obtain the optimal path in the strong disorder limit, we present the following theoretical argument. It has been shown [Braunstein *et al.*, 2001; Cieplak *et al.*, 1996] that the optimal path for $a \rightarrow \infty$ between two nodes A and B on the network can be obtained by the bombing algorithm described in Section II D.

This algorithm is based on randomly removing links. Since randomly removing links is a percolation process, the optimal path must be on the percolation backbone connecting A and B. We can explore the network starting with node A by Dijkstra's algorithm, sequentially creating burning shells of chemical distance n from the node A. Alternatively we can think of the n-th shell as of n-th generation of descendants of a parent A in a branching process. The random network consisting of a large number of nodes $N \to \infty$ and small average degree $\langle k \rangle \ll N$, has a tree-like local structure with no loops, since the probability that a node we randomly chose by an outgoing link has been already visited is less than $\langle k \rangle^n / N$, which remains negligible for $n < \ln N / \ln \langle k \rangle$.

As we remove links by the bombing algorithm, the average degree of remaining nodes decreases, and the role of loops decreases. Thus finite loops play no role in determining the properties of the optimal path. In fact, connecting the nodes A and B by an optimal path is equivalent to connecting each of them to a very distant shell on a corresponding Cayley tree. As the fraction $q = 1 - p$ of remaining links decreases, we reach the percolation threshold at which removal of a next link destroys the connectivity with a very high probability. Note that if we select weights of the links $\tau_i = \exp(ar_i)$, where r_i is uniformly distributed on $[0, 1]$, the fraction of remaining bonds, p, is equal to r_i of the next link we will remove.

A.   Distribution of the maximal weight on the optimal path

In order to further develop this analogy, we will show that the distribution of the maximal random number $r_{\max}$ along the optimal path[5] can be expressed in terms of the order parameter $P_\infty(p)$ in the percolation problem on the Cayley tree, where $P_\infty(p)$ is the probability that a randomly chosen site on the Cayley tree has infinite number of generations of descendants or, in other words, belongs to the infinite cluster.

If the original graph has a degree distribution $P(k)$, the probability that we reach a node with a degree k by following a randomly chosen link on the graph, is equal to $kP(k)/\langle k \rangle$, where $\langle k \rangle$ is the average degree. This is because the probability of reaching a given node by following a randomly chosen link is proportional to the number of links, k, of that node and $\langle k \rangle$ comes from normalization. Also, if we arrive at a node with degree k, the total number of outgoing branches is $k - 1$. Therefore, from the point of view of the Cayley tree, the probability p_{k-1} to arrive at a node with $k - 1$ outgoing branches by following a randomly

16

chosen link is

$$p_{k-1} = kP(k)/\langle k \rangle. \tag{5}$$

In the asymptotic limit, $N \to \infty$, when the optimal path between the two nodes is very long, the probability distribution for the maximal weight link can be obtained from the following analysis. Let us assume that the probability of *not* reaching $n-th$ generation starting from a randomly chosen link of the Cayley tree whose links exist with a probability p, is Q_n. Suppose this link leads to a node whose outgoing degree is 2. Then the probability that starting from this link, we will not reach n generations of its descendants is the sum of three terms:

1. The probability that both outgoing links do not exist is equal to $(1-p)^2$

2. The probability that both outgoing links exist, but they do not have $n-1$ generations of descendants is equal to $p^2 Q_{n-1}^2$

3. The probability that only one of the two outgoing links exist but it does not have $n-1$ generations of descendants is equal to $2(1-p)pQ_{n-1}$

Therefore, in this case

$$Q_n = (1-p)^2 + p^2 Q_{n-1}^2 + 2(1-p)pQ_{n-1}, \tag{6}$$

which on simplification becomes

$$Q_n = ((1-p) + pQ_{n-1})^2. \tag{7}$$

Following this argument for the case when our link leads to a node with m outgoing links, the probability that starting from this node, we can not reach n generations, is

$$Q_n = ((1-p) + pQ_{n-1})^m. \tag{8}$$

In the case of a Cayley tree with a variable degree, we must incorporate a factor p_{k-1} given by Eq.(5) which accounts for the probability that the node under consideration has $k-1$ outgoing edges and sum up over all possible values of k. Thus for a conducting link on the Cayley tree, the probability that it does not have descendants in generation n can be obtained by applying a recursion relation

$$Q_l = \sum_{k=1}^{\infty} P(k)k((1-p) + pQ_{l-1})^{k-1}/\langle k \rangle \tag{9}$$

for $l = 1, 2, ..., n$ with the initial condition $Q_0 = 0$, which indicates that a given link is always present in generation zero of its descendants.

For a random graph, a randomly chosen node has k outgoing edges with the original probability $P(k)$. Thus it has a slightly different probability $Q_n(p)$ of not having descendants in its nth generation:

$$\tilde{Q}_n = \sum_{k=0}^{\infty} P(k)((1-p) + pQ_{n-1})^k. \tag{10}$$

It is convenient to introduce the generating function of the original degree distribution

$$\tilde{G}(x) \equiv \sum_{k=1}^{\infty} P(k)x^k \tag{11}$$

and the generating function of the degree distribution of the Cayley tree

$$G(x) \equiv \sum_{k=1}^{\infty} \frac{kP(k)}{\langle k \rangle} x^{k-1}, \tag{12}$$

where x is an arbitrary complex variable. Using the normalization conditions for the probabilities $\sum_{k=0}^{\infty} P(k) = 1$, it easy to see that $\tilde{G}(1) = 1$. Taking into account that $\langle k \rangle = \sum_{k=0}^{\infty} kP(k)$ we have $\langle k \rangle = d\tilde{G}/dx|_{x=1} = \tilde{G}'(1)$ and hence $\tilde{G}(x)$ and $G(x)$ are connected by a relation

$$G(x) = \tilde{G}'(x)/\tilde{G}'(1). \tag{13}$$

For any degree distribution $P(k) \to 0$, as $k \to \infty$ and thus both functions are analytic functions of x and have a convergence radius $R \geq 1$. Since $P(k) > 0$, these functions and all their derivatives are monotonically increasing functions on an interval $[0, 1)$. For the ER networks, the degree distribution is Poisson given by: $P(k) = \langle k \rangle^k \exp^{-\langle k \rangle}/k!$, hence $\tilde{G}(x) = G(x) = \exp[\langle k \rangle(x - 1)]$. For scale free distribution, $P(k) \sim k^{-\lambda}$, hence $\tilde{G}(x)$ is proportional to Riemann ζ-function, $\zeta_\lambda(x)$.

If we denote by $f_n(p)$, the probability that starting at a randomly chosen conducting link we can reach, or survive up to, the n-th generation, then

$$f_n = 1 - Q_n(p) \tag{14}$$

and by $\tilde{f}_n(p)$, the probability that a randomly chosen node has at least n generation of descendants,

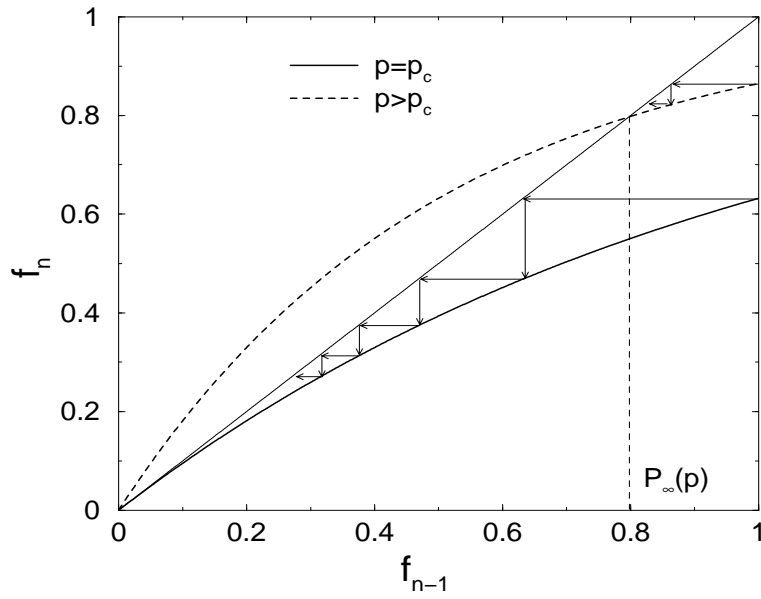$$\tilde{f}_n = 1 - \tilde{Q}_n(p) \tag{15}$$

18

FIG. 2: The iterative process of solving equation (18). The thin straight line $y = x$ represents the left hand side. The bold curve represents the right hand side (r.h.s) for $p = p_c$, at which the r.h.s. is tangential to $y = x$ at the origin. The dashed curve represents r.h.s. for $p > p_c$. Both cases are computed for the Poisson degree distribution with $\langle k \rangle = 2$, so r.h.s of Eq. (18) is given by $1 - \exp(-2px)$. The arrows represent iterations starting from $f_0 = 1$ (the starting link belongs to generation 0). It is clear that the convergence of the iterations is very fast (exponential) for $p \neq p_c$, while it is very slow (power law) for $p = p_c$.

then

$$f_n = 1 - G(1 - pf_{n-1}) \tag{16}$$

and

$$\tilde{f}_n = 1 - \tilde{G}(1 - pf_{n-1}). \tag{17}$$

The sequence of iterations (16) is visualized (See Fig. 2) as a process of solving the equation

$$x = 1 - G(1 - px) \tag{18}$$

by an iteration method. Obviously, this equation has at least one root $x_0 = 1$. But if the derivative of the right hand side, $[1 - G(1-px)]'|_{x=0} = pG'(1) > 1$, we will have another root $0 < x_1 \leq 1$. This root has a physical meaning of a probability $P_\infty(p)$ that a randomly selected conducting link is connected to infinity (See also [Cohen $et\ al.$, 2000]). For $p > 1/G'(1)$, the iterations will converge to this root, while for $p \leq 1/G'(1)$, the iterations will converge to
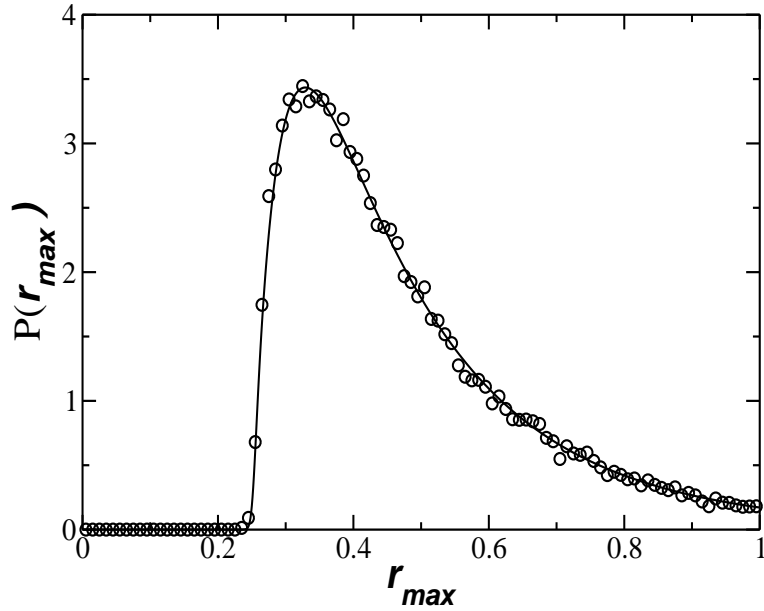
19

FIG. 3: The probability distribution of the maximal random number $r_{\max}$ along the optimal path obtained using simulations on a random graph with $\langle k \rangle = 4$ and using the analytical method on a Cayley tree with Poisson degree distribution and $\langle k \rangle = 4$. The simulations involve 100000 network realizations and are carried out on a network of 65536 nodes. The values of l_{opt} for this network lie in the range $40 < l_{\mathrm{opt}} < 120$ (After [Braunstein et $al.$, 2004]).

$P_\infty(p) = 0$. Thus

$$p_c \equiv \frac{1}{G'(1)} = \frac{\langle k \rangle}{\langle k^2 \rangle - \langle k \rangle} = \frac{1}{\kappa - 1} \tag{19}$$

has a meaning of the percolation threshold above which there is a finite probability to reach the infinity. Using this equation we can derive the condition $\kappa < 2$ to stop bombing in the process of obtaining IIC. Indeed $\kappa < 2$ indicates that equation (18) has only one trivial solution $x_0 = 0$ even for $p = 1$. This means that all the clusters in this network are finite. If $\kappa > 2$, $p_c < 1$ accordingly $P_\infty(1) > 0$, i.e. the infinite cluster does exist. The condition $\kappa = 2$ corresponds to $p_c = 1$ which means that any further link removal will produce a network in which $P_\infty(1) = 0$,i.e. the network with only finite clusters, while at $p = 1$, the infinite cluster is incipient.

The probability that a randomly chosen node is connected to infinity can be determined as

$$\tilde{P}_\infty(p) = 1 - \tilde{G}(1 - pP_\infty(p)), \tag{20}$$

where $P_\infty(p)$ is a non-trivial solution of Eq. (18). For some degree distributions including

20

Poisson distribution, $\tilde{P}_\infty(1) < 1$. This indicates that a randomly chosen node on the original network may not belong to the giant component of the network. In fact, the optimal path between nodes A and B exists if both belong to the giant component. Provided that A and B both belong to the giant component, the probability that they are still connected when the fraction $1 - p$ of bonds is removed is

$$\Pi(p) = \left(\frac{\tilde{P}_\infty(p)}{\tilde{P}_\infty(1)} \right)^2 . \tag{21}$$

Translating this condition to the bombing algorithm of generating an optimal path, $\Pi(p)$ is the probability that the maximum random number along the optimal path $r_{\max} \leq p$. Indeed, $\Pi(p)$ is the probability that when only a fraction p of links remains the connectivity between A and B still exists. Hence $r_{\max} \leq p$. Thus, $\Pi(r_{\max})$ is the cumulative distribution of $r_{\max}$. The probability density of $r_{\max}$ is thus equal to the derivative of $\Pi(p)$ with respect to p:

$$P(r_{\max}) = \frac{d}{dp}\Pi(p)|_{p=r_{\max}}. \tag{22}$$

In Fig. 3 we plot two curves. The curve with symbols is the probability distribution of $r_{\max}$ in a strongly disordered ER graph with $\langle k \rangle = 4$ obtained by simulations. The line shows the same probability distribution obtained using (Eq. (22)) for a Poisson degree distribution with $\langle k \rangle = 4$. The curves coincide very well, indicating the excellent agreement between the theoretical analysis and simulations.

B.   Distribution of the cluster chemical length at percolation threshold

Figure 2 illustrates the convergence of the probability of the random link to have descendants in the n-th generations. The difference $P(n) = f_n - f_{n+1}$ is the probability that the last generation of the descendants of this link is n. In percolation language, it is the probability distribution of the cluster chemical length $\ell = n$. In order to find, how $f_n \to 0$ when $p = p_c$, we can expand equation (16) in Taylor series at $f_n = 0$. For ER networks, $G(x)$ has all the derivatives at $x = 1$, thus (16) can be presented as

$$f_n = pG'(1)f_{n-1} - \frac{1}{2}p^2 G''(1)f_{n-1}^2 + O(f_{n-1}^2). \tag{23}$$

For SF graphs with $\lambda > 4$, $G''(1)$ also exists, thus the above equation holds. For $3 < \lambda < 4$ the second derivative does not exist, however using the Tauberian theorem which relates the

speed of the decay of the coefficients $P(k) \sim k^{-\mu}$ of the power series and the behavior of its singularity at the convergence radius: $G_s(x) \sim (1-x)^{\mu-1}$ we can write:

$$f_n = pG'(1)f_{n-1} - cf_{n-1}^{\lambda-2} + O(f_{n-1}^{\lambda-2}), \qquad (24)$$

where c is some positive coefficient.

As $\lambda \to 3$, $G'(1) \to \infty$ and hence, according to Eq.(19) $p_c \to 0$. This means that for SF networks with $\lambda \le 3$, percolation approach breaks down. However, for finite networks, it is unlikely to have a degree larger than $N^{1/(\lambda-1)}$. This fact is obvious since when one generates random degrees with probability distribution $P(k)$, one produces random numbers x uniformly distributed on a interval between 0 and 1, and compute $k = f(x)$, where $f(x)$ satisfies the equation $x = \sum_{f(x)}^{\infty} P(k) \sim f(x)^{-\lambda+1}$. Thus the largest k corresponds to the smallest x. Generating N random numbers is equivalent to throwing N points on an interval $[0,1]$ which divide this interval into $N+1$ segments whose lengths are identically distributed with an exponential distribution. Thus the average value of the smallest x is equal to $1/(N+1)$. Accordingly the average value of the largest k can be approximated as $k_{\max} = f(1/(N+1)) \sim N^{1/(\lambda-1)}$ [Cohen *et al.*, 2000]. Thus replacing summation by integration up to $k_{\max}$ in the expression for $G'(1) \approx \int^{k_{\max}} k^{-\lambda+2}dk \sim k_{max}^{3-\lambda} = N^{(3-\lambda)/(\lambda-1)}$. Hence for $2 < \lambda < 3$ [Cohen *et al.*, 2000].

$$p_c \sim N^{(\lambda-3)/(\lambda-1)}. \qquad (25)$$

When $p < p_c$, $f_n \sim (p/p_c)^n$, i.e. the convergence is exponential. When $p = p_c$, we will seek the solution of the above recursion relations in a power law form: $f_n \sim n^{-\theta}$. Expanding them in powers of n^{-1}, and equating the leading powers, we have $\theta + 1 = \theta(\lambda - 2)$, from which we obtain

$$f_n \sim n^{-1/(\lambda-3)}, \qquad (26)$$

or

$$P(\ell) = f_\ell - f_{\ell+1} \sim \ell^{-\tau_\ell}, \qquad (27)$$

where [Cohen *et al.*, 2002; Cohen *et al.*, 2002]

$$\tau_\ell = \begin{cases} 2, \ \lambda > 4 \qquad \text{ER} \\ \frac{1}{(\lambda-3)} + 1, \ 3 < \lambda \le 4 \end{cases}. \qquad (28)$$

22

The probability that a randomly selected *node* has exactly ℓ generations of descendants is equal to

$$\tilde{P}(\ell) = \tilde{f}_\ell - \tilde{f}_{\ell+1} = \tilde{G}(1 - pf_\ell) - \tilde{G}(1 - pf_{\ell-1}) \sim \langle k \rangle p(f_\ell - f_{\ell-1}). \tag{29}$$

Thus it is characterized by the same τ_ℓ as $P(\ell)$.

Taylor expansions (23) and (24) can be used to derive the behavior of $P_\infty(p)$ as $p \to p_c$ by letting $f_n = f_{n-1} = P_\infty(p)$ and solving the resulting equations with a leading term accuracy:

$$P_\infty(p) = (p - p_c)^\beta, \tag{30}$$

where [Cohen *et al.*, 2000]

$$\beta = \begin{cases} 1, & \lambda > 4 \qquad \text{ER} \\ \lambda - 3, & 3 < \lambda \le 4 \end{cases}. \tag{31}$$

C. Distribution of the cluster sizes at percolation threshold

Using the generating functions [Cohen *et al.*, 2002; Cohen *et al.*, 2002; Callaway *et al.*, 2000], one can also find the distribution of the clusters sizes, $P(s)$, connected to a randomly selected *link*. For simplicity, let us again consider a link (conducting with probability p) leading to a node of a degree $k = 3$, so it has only two outgoing links. The probability that this link is connected to a cluster consisting of s nodes obeys the following relations

$$P(s) = p \sum_{k+l=s-1} P(k)P(l) \tag{32}$$

for $s > 0$ and $P(0) = 1 - p$. Introducing the generating function of the cluster size distribution $H(x) = \sum_0^\infty P(s)x^s$, we have: $H(x) = 1 - p + xpH^2(x)$. In a general Cayley tree with an arbitrary degree distribution we have:

$$H(x) = 1 - p + xpG(H(x)). \tag{33}$$

This equation defines the behavior of $H(x)$ for $x \to 1$, and thus via the Tauberian theorem defines the asymptotic behavior of its coefficients $P(s)$. Note that $H(1)$ is the cumulative probability of all finite clusters. Thus $(1 - H(1)) = pP_\infty(p)$ is the probability that a randomly selected link conducting with probability p is connected to the infinity and Eq.(33) becomes equivalent to Eq. (18) for $P_\infty(p)$.

23

Introducing $\delta_x = 1 - x$ and $\delta_H = 1 - H(x)$ and expanding $G(x)$ around $x = 1$ at percolation threshold $p = 1/G'(1)$, we have $\delta_H \delta_x + p \delta_x = c x \delta_H^{\lambda-2} + O(\delta_H^{\lambda-2})$ which yields $\delta_H \sim \delta_x^{1/(\lambda-2)}$. Using the Tauberian theorem we conclude [Cohen *et al.*, 2002; Cohen *et al.*, 2002]:

$$P(s) \sim s^{-\tau_s}, \tag{34}$$

where

$$\tau_s = \begin{cases} 3/2, \ \lambda > 4 \qquad \text{ER} \\ \frac{1}{\lambda-2} + 1, \ 3 < \lambda \le 4 \end{cases}. \tag{35}$$

Analogous considerations suggest that the probabilities $\tilde{P}(s)$ that a randomly selected *node* belongs to the cluster of size s produce the generating function $\tilde{H}(x) = \tilde{G}(H(x))$. Since for $\lambda > 3$, $\tilde{G}''(1) < \infty$, the singularity of $\tilde{H}(x)$ for $x \to 1$ is of the same order as the singularity of $H(x)$ and thus its coefficients, $\tilde{P}(s)$, also decay as $s^{-\tau_s}$.

Following [Stauffer & Aharony, 1994], we will show that the distribution of all the disconnected clusters in a network scales as $P_{all}(s) = \tilde{P}(s)/s \sim s^{-\tau_s+1}$. Indeed, let us select a random node in this network. The number of nodes belonging to the clusters of size s is $N s P_{all}(s) / \sum_1^\infty s P_{all}(s) = N s P_{all}(s)/\langle s \rangle$. Thus, $\tilde{P}(s) = s P_{all}(s)/\langle s \rangle$.

If we have a network of N nodes, the size of the largest cluster S is determined by the relation $\sum_{s=S}^\infty P_{all}(s) \sim 1/N$, which becomes clear if we describe a concrete realization of the cluster sizes by throwing $N/\langle s \rangle$ random points representing clusters under the curve $P_{all}(s)$. The average area corresponding to each of these points is $1/N$ and the area corresponding to the rightmost point representing the largest cluster is $\sum_{s=S}^\infty P_{all}(s) \sim S^{-\tau_s}$. Thus the largest cluster (which coincides with IIC) in the network of N nodes scales as

$$S \sim N^{1/\tau_s}. \tag{36}$$

For ER graphs, the relation $S \sim N^{2/3}$ has been derived in a classical work [Erdős & Rényi, 1959].

IV. SCALING OF THE LENGTH OF THE OPTIMAL PATH IN STRONG DISORDER

The relations obtained in the previous subsections allow us to determine the scaling of the average optimal path length in a network of N nodes. When during bombing, we

24

reach percolation threshold, we have targeted only a tiny fraction of links (or nodes) on the optimal path, with $r_{max} > p_c$ which we have to restore, because their removal would destroy the connectivity. The majority of the links on the optimal path remains intact. All of them belong to the remaining percolation clusters which at percolation threshold has a tree like structure with no loops. At this point, the optimal path coincides with the shortest path, which is uniquely determined. We will describe this situation in detail in SectionVI. With high probability, the optimal path between any two nodes A and B goes through the largest cluster at the percolation threshold. Thus its length must scale as the chemical length of the largest percolation cluster [Braunstein et al., 2003]. Assuming a power law relation between the cluster size s and its chemical dimension ℓ, $s = \ell^{d_\ell}$, and using the fact that both of the quantities have power law distributions $P(\ell)d\ell = \tilde{P}(s)ds$, we have $\ell^{-\tau_\ell} = \ell^{-d_\ell \tau_s + d_\ell - 1}$. Thus [Barrat et al., 2004]

$$d_\ell = (\tau_l - 1)/(\tau_s - 1). \tag{37}$$

Therefore, $S \sim \ell_{opt}^{d_\ell}$ and using (36) we have $\ell_{opt} \sim S^{1/d_\ell} \sim N^{\nu_{opt}}$, where

$$\nu_{opt} = 1/(d_\ell \tau_s). \tag{38}$$

Using Eqs. (35) and (28) for τ_s and τ_ℓ respectively, we have

$$\nu_{opt} = \begin{cases} 1/3, \ \lambda > 4, \quad \text{ER} \\ (\lambda - 3)/(\lambda - 1), \ 3 < \lambda \leq 4 \end{cases}. \tag{39}$$

Note that $\lambda = 4$ corresponds to the special case when $G''(1)$ diverges, in this case the Tauberian theorem predicts logarithmic corrections, and hence we expect $\ell_{opt} \sim N^{1/3}/\ln N$ for $\lambda = 4$.

We review above the exact results for the Cayley tree, from which using heuristic arguments we have derived the scaling relation between the average length of the optimal path and the number of nodes in the network. Now we will show how the same predictions can be obtained using general percolation theory. We will also present numerical data supporting our heuristic arguments. We begin by considering the ER graph. At criticality, it is equivalent to percolation on the Cayley tree or percolation at the upper critical dimension $d_c = 6$. For the ER graph, we derived above that the mass of the IIC, S, scales as $N^{2/3}$ [Erdős & Rényi, 1959]. This result can also be obtained in the framework of percolation theory for $d_c = 6$. Since $S \sim R^{d_f}$ and $N \sim R^d$ (where d_f is the fractal dimension and R the spatial
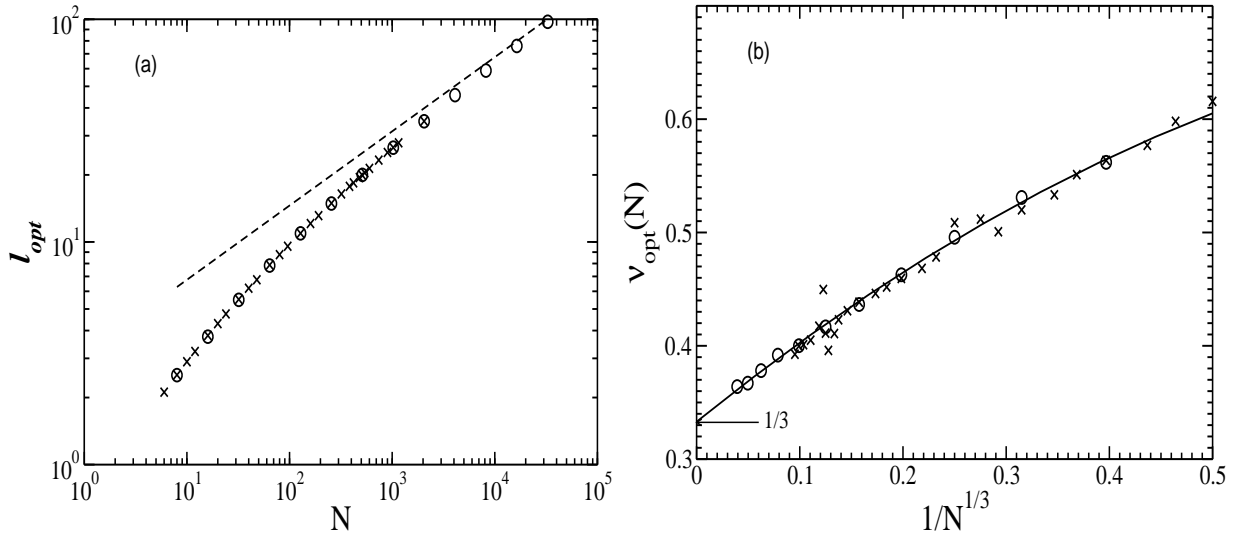
FIG. 4: (a) Plot of ℓ_{opt} as a function of N in double logarithmic scale for the optimal path length in strong disorder using the two numerical methods discussed in the text: (i) results obtained using the "bombing" approach ($\circ$) and (ii) results obtained using the ultrametric approach ($\times$). The dashed line shows the slope $1/3$. (b) Successive slopes $\nu_{\text{opt}}(N)$ as a function of $1/N^{1/3}$ for the optimal path length in strong disorder using the two methods described in the text. The symbols denote the same as in (a). The dashed line is the quadratic fitting of the results showing that the extrapolated value of the effective exponent in the limit $N \to \infty$ approaches $1/3$. This result coincides with our theoretical value $\nu_{opt} = 1/3$ asymptotically (After [Braunstein *et al.*, 2003; Havlin *et al.*, 2005]).

diameter of the cluster), it follows that $S \sim N^{d_f/d}$ and for $d_c = 6$, $d_f = 4$ [Bunde & Havlin, 1996] we obtain $S \sim N^{2/3}$ [Watts, 2003].

It is also known [Bunde & Havlin, 1996] that, at criticality, at the upper critical dimension, the average shortest path length $\ell_{\text{min}} \sim R^2$, like a random walk and therefore $S \sim \ell_{\text{min}}^{d_\ell}$ with $d_\ell = 2$. Thus

$$\ell_{\text{min}} \sim \ell_{\text{opt}} \sim S^{1/d_\ell} \sim N^{2/3d_\ell} \sim N^{\nu_{\text{opt}}}, \tag{40}$$

where $\nu_{\text{opt}} = 2/3d_\ell = 1/3$.

For SF networks, we can also use the percolation results at criticality. It was found [Cohen *et al.*, 2002; Cohen *et al.*, 2002] (see Sec. III) that $d_\ell = 2$ for $\lambda > 4$, $d_\ell = (\lambda - 2)/(\lambda - 3)$ for $3 < \lambda < 4$, $S \sim N^{2/3}$ for $\lambda > 4$, and $S \sim N^{(\lambda-2)/(\lambda-1)}$ for $3 < \lambda \leq 4$. Hence, we conclude

that

$$\ell_{\min} \sim \ell_{\mathrm{opt}} \sim \begin{cases} N^{1/3} & \lambda > 4 \\ N^{(\lambda-3)/(\lambda-1)} & 3 < \lambda \le 4 \end{cases}. \tag{41}$$

Thus $\nu_{opt} = 1/3$ for ER and SF with $\lambda > 4$, and $\nu_{opt} = (\lambda-3)/(\lambda-1)$ for SF with $3 < \lambda < 4$. Since for SF networks with $\lambda > 4$ the scaling behavior of ℓ_{opt} is the same as for ER graphs and for $\lambda < 4$ the scaling is different, we can regard SF networks as a generalization of ER graphs.

Next we describe the details of the numerical simulations and show that the results agree with the above theoretical predictions. We perform numerical simulations in the strong disorder limit by the method described in Section II D for ER and SF networks. We also perform additional simulations for the case of strong disorder on ER networks using the ultrametric optimization algorithm (see Section II C) and find results identical to the results obtained by randomly removing links. In Fig. 4(a) we show a double logarithmic plot of ℓ_{opt} as a function of N for ER graphs. To evaluate the asymptotic value for ν_{opt} we use for both approaches successive slopes, defined as the successive slopes [Braunstein *et al.*, 2001] of the values on Fig. 4. One can see from Fig. 4(b) that their value approaches $1/3$ when $N \gg 1$, supporting Eq. (40).

The theoretical considerations [Eqs. (40) and (41)] predict that SF graphs with $\lambda > 4$, are similar to ER with $\ell_{\mathrm{opt}} \sim N^{1/3}$, while for SF graphs with $3 < \lambda < 4$, $\ell_{\mathrm{opt}} \sim N^{(\lambda-3)/(\lambda-1)}$. Figure 5a shows data from numerical simulations supporting the linear behavior of ℓ_{opt} versus $N^{1/3}$ for $\lambda \ge 4$. The quality of the linear fit becomes poor for $\lambda \to 4$. At this value, there are corrections probably due to logarithmic divergence of the second moment of the degree distribution, i.e., $\ell_{\mathrm{opt}} \sim N^{1/3}/\ln N$ (see Fig. 5b). Figure 5c shows results of simulations supporting the asymptotic linear behavior of ℓ_{opt} versus $N^{(\lambda-3)/(\lambda-1)}$ for $3 < \lambda \le 4$. Theoretically, as $\lambda \to 3$, $\nu_{\mathrm{opt}} = (\lambda-3)/(\lambda-1) \to 0$, and thus one can expect for $\lambda = 3$ a logarithmic N dependence of ℓ_{opt}. Indeed, for $2 < \lambda < 3$ our numerical results for the strong disorder limit suggest that ℓ_{opt} scales slower than a power law with N but slightly faster than $\ln N$. The numerical results can be fit to $\ell_{\mathrm{opt}} \sim (\ln N)^{\lambda-1}$ (see Fig. 5d). Note that the correct asymptotic behavior may be different and this result may represents only a crossover regime. The exact nature of the percolation cluster at $\lambda < 3$ is not clear yet, since in this regime the transition does not occur at a finite (non zero) critical threshold [Cohen *et al.*, 2000]. We obtain similar results for SF networks where the weights are associated
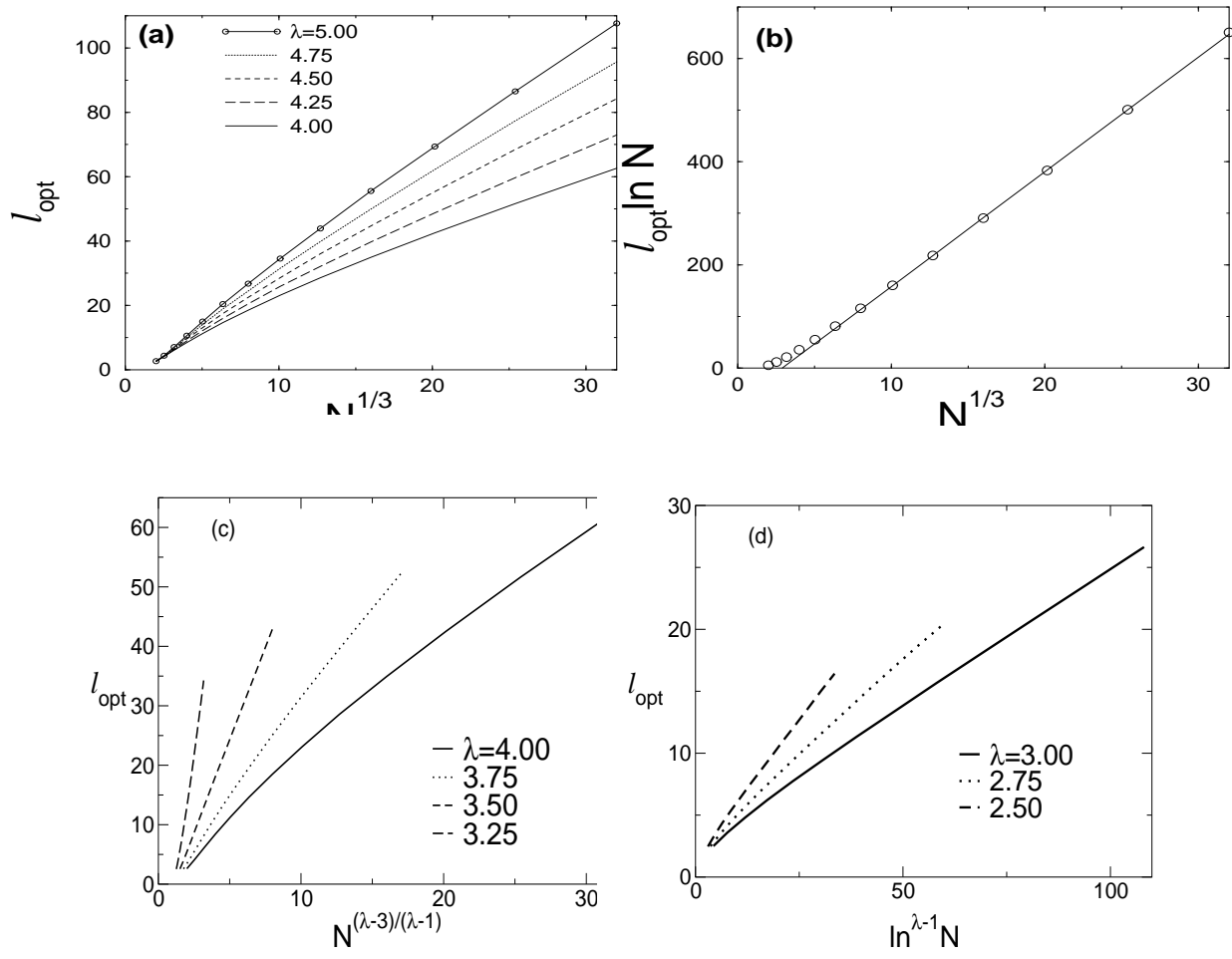
FIG. 5: Results of numerical simulations. (a) The dependence of ℓ_{opt} on $N^{1/3}$ for $\lambda \geq 4$. (b) The dependence of $\ell_{opt}/\ln N$ on $N^{1/3}$ for $\lambda = 4$. (c) The dependence of ℓ_{opt} on $N^{(\lambda-3)/(\lambda-1)}$ for $3 < \lambda < 4$. (d) The dependence of ℓ_{opt} on $\ln N$ for $\lambda \leq 3$ (After [Braunstein et $al.$, 2003; Havlin et $al.$, 2005]).

with nodes instead of links.

V. SCALING OF THE LENGTH OF THE OPTIMAL PATH IN WEAK DISORDER

When $a = 1/kT \to 0$, all the τ_i essentially contribute to the total cost. Thus $T \to \infty$ (very high temperatures) corresponds to weak disorder limit. We expect that the optimal path length in the weak disorder case will not be considerably different from the shortest path, as found also for regular lattices [Smailer et $al.$, 1993] and random graphs [van der

Hofstad *et al.*, 2001]. Thus we expect that the scaling for the shortest path will also be valid for the optimal path in weak disorder, but with a different prefactor depending on the details of the graph and on the type of disorder. We simulate weak disorder by selecting $0 \leq \tau_i < 1$ from a uniform distribution. To compute ℓ_{opt} we use the Dijkstra algorithm (See Section II B)[Cormen *et al.*, 1990]. The scaling of the length of the optimal path in WD for ER, is shown in Fig. 6(a). Here we plot ℓ_{opt} as a function of $\ln N$ for $\langle k \rangle = 4$. The weak disorder does not change the scaling behavior of ℓ_{opt} on ER compared to ℓ_{min}, only the prefactor.
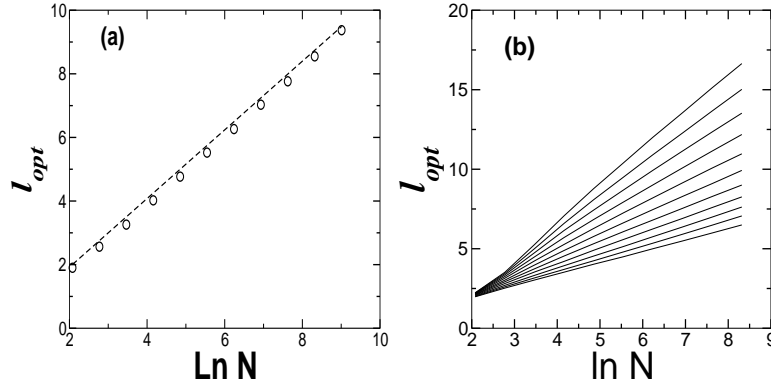

FIG. 6: Results of numerical simulations. (a) The linear dependence of ℓ_{opt} on $\ln N$ for ER graphs in the weak disorder case for $< k > = 4$. The dashed line is used as a guide to show the linear dependence. (b) The dependence of ℓ_{opt} on $\ln N$ for SF graphs in the weak disorder case for various values of λ. The different curves represent different values of λ from 2.5 (bottom) to 5 (top). (After [Sreenivasan *et al.*, 2004; Sreenivasan *et al.*, 2005].)

For SF networks, the behavior of the optimal path in the weak disorder limit is shown in Fig. 6(b) for different degree distribution exponents λ. Here we plot ℓ_{opt} as a function of $\ln N$. All the curves seem to have linear asymptotes. This result is analogous to the behavior of the shortest path $\ell_{min} \sim \ln N$ for $3 < \lambda < 4$ and ER. Note, however, that for $2 < \lambda < 3$, ℓ_{min} scale as $\ln \ln N$ [Cohen & Havlin, 2003]. Thus, ℓ_{opt} is significantly larger and scales as $\ln N$ (Fig. 3b). Thus, weak disorder does not change the universality class of the length of the optimal path except in the case of "ultra-small" worlds $2 < \lambda < 3$, where $\ell_{opt} \sim \exp(\ell_{min})$, and the networks become small worlds.

VI. CROSSOVER FROM WEAK TO STRONG DISORDER

A. Exponential Disorder

Consider the case of finite a ($T > 0$). In this case we expect a crossover in the length of the optimal path (or the system size N) from strong disorder behavior to weak disorder depending on the value of a. In order to study this crossover we have to use an implementation of disorder that can be tuned to realize narrow distributions of link weights (WD) as well as broad distributions of link weights (SD). The procedure that we adopt to implement the disorder is as follows [Cieplak *et al.*, 1996; Porto *et al.*, 1999; Braunstein *et al.*, 2001; Braunstein *et al.*, 2003] (see Sec. IV A). Assign to each link i of the network a random number r_i, uniformly distributed between 0 and 1. For the analogy with the thermally activated process described in Sec. IV the r_i play the role of the energy barriers. The transit time or cost associated with link i is then $\tau_i \equiv \exp(ar_i)$, where a controls the strength of disorder i.e., the broadness of the distribution of link weights. The limit $a \to \infty$ is the strong disorder limit, where a single link dominates the cost of the path. For d-dimensional lattices of size L, the crossover is found [Cieplak *et al.*, 1996; Porto *et al.*, 1999] to behave as

$$\ell_{opt} \sim \begin{cases} L^{d_{\mathrm{opt}}}, & L \ll a^{\nu}; \\ L, & L \gg a^{\nu}. \end{cases} \tag{42}$$

where ν is the percolation correlation exponent [Strelniker *et al.*, 2004; Wu *et al.*, 2005]. For $d = 2$, $d_{\mathrm{opt}} \approx 1.22$ and for $d = 3$, $d_{\mathrm{opt}} \approx 1.44$ [Cieplak *et al.*, 1996; Porto *et al.*, 1999]. Here we show [Sreenivasan *et al.*, 2004] that for any network of size N and any finite a, there exists a crossover network size $N^*(a)$ such that for $N \ll N^*(a)$ the scaling properties of the optimal path are in the strong disorder regime, while for $N \gg N^*(a)$ the typical optimal paths are in the weak disorder regime. We evaluate below the function $N^*(a)$.

In general, the average optimal path length $\ell_{opt}(a)$ in a weighted network depends on a as well as on N. In the following we use instead of N the min-max path length ℓ_∞ which is related to N as $\ell_\infty \equiv \ell_{\mathrm{opt}}(\infty) \sim N^{\nu_{\mathrm{opt}}}$ [Eqs.(40) and (41)] and hence N can be expressed in terms of ℓ_∞,

$$N \sim \ell_\infty^{1/\nu_{\mathrm{opt}}}. \tag{43}$$

Thus, for finite a, $\ell_{\mathrm{opt}}(a)$ depends on both a and ℓ_∞. We expect a crossover length $\ell^*(a)$, which corresponds to the crossover network size $N^*(a)$, such that (i) for $\ell_\infty \ll \ell^*(a)$, the

scaling properties of $\ell_{\rm opt}(a)$ are of the strong disorder regime, and (ii) for $\ell_\infty \gg \ell^*(a)$, the scaling properties of $\ell_{\rm opt}(a)$ are of the weak disorder regime. In Fig. 7, we show a schematic representation of the changes of the optimal path as the network size increases.
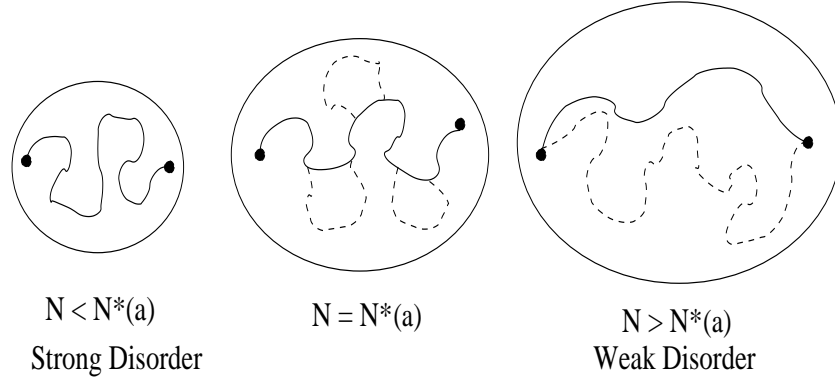

N < N*(a)
Strong Disorder

N = N*(a)

N > N*(a)
Weak Disorder

FIG. 7: Schematic representation of the transition in the topology of the optimal path with system size N for a given disorder strength a. The solid line shows the optimal path at a finite value of a connecting two nodes indicated by the filled circles. The portion of the min-max path that is distinct from the optimal path is indicated by the dashed line. (a) For $N \ll N^*(a)$ (i.e. $\ell_\infty \ll \ell^*(a)$), the optimal path coincides with the min-max path, and we expect the statistics of the SD limit. (b) For $N = N^*(a)$ (i.e. $\ell_\infty = \ell^*(a)$), the optimal path starts deviating from the min-max path. (c) For $N \gg N^*(a)$ (i.e. $\ell_\infty \gg \ell^*(a)$), the optimal path has almost no links in common with the min-max path, and we expect the statistics of the WD limit (After [Sreenivasan *et al.*, 2004; Sreenivasan *et al.*, 2005]).

In order to study the transition from strong to weak disorder, we introduce a measure which indicates how close or far the disordered network is from the limit of strong disorder. A natural measure is the ratio

$$W(a) \equiv \frac{\ell_{\rm opt}(a)}{\ell_\infty}. \tag{44}$$

Using the scaling relationships between $\ell_{\rm opt}(a)$ and N in both regimes, and $\ell_\infty \sim N^{\nu_{\rm opt}}$, we get

$$\ell_{\rm opt}(a) \sim \begin{cases} \ell_\infty \sim N^{\nu_{\rm opt}} & \text{[SD]} \\ \ln \ell_\infty \sim \ln N & \text{[WD]}. \end{cases} \tag{45}$$

¿From Eq. (44) and Eq. (45) it follows,

$$W(a) \sim \begin{cases} \text{const.} & \text{[SD]} \\ \ln \ell_\infty / \ell_\infty & \text{[WD]}. \end{cases} \tag{46}$$

31

We propose the following scaling Ansatz for $W(a)$,

$$W(a) = F\left(\frac{\ell_\infty}{\ell^*(a)}\right), \tag{47}$$

where

$$F(u) \sim \begin{cases} \text{const.} & u \ll 1 \\ \ln(u)/u & u \gg 1 \end{cases}, \tag{48}$$

with

$$u \equiv \frac{\ell_\infty}{\ell^*(a)}. \tag{49}$$

We now develop analytic arguments [Sreenivasan et al., 2004] to obtain the dependence of the crossover length ℓ^* on the disorder strength a. These arguments will also give a clearer picture about the nature of the transition of the optimal path with disorder strength.

We begin by making few observations about the min-max path. In Fig. 8 we plot the average value of the random numbers r_n on the min-max path as a function of their rank n ($1 \leq n \leq \ell_\infty$) for ER networks with $\langle k \rangle = 4$ and for SF networks with $\lambda = 3.5$. This can be done for a min-max path of any length but in order to get good statistics we use the most probable min-max path length. We call links with $r \leq p_c$ "black" links, and links with $r > p_c$ "gray" links, following the terminology of Ioselevich and Lyubshin [Ioselevich & Lyubshin, 2004] where p_c is the percolation threshold of the network [Cohen et al., 2000].
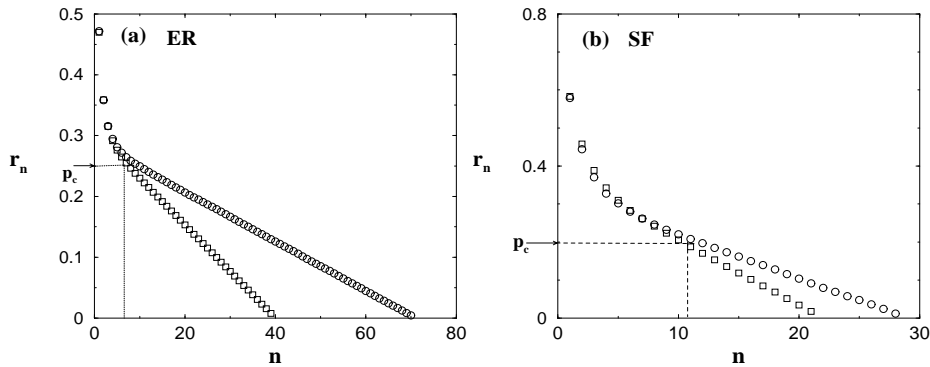

FIG. 8: Dependence on rank n of the average values of the random numbers r_n along the most probable optimal path for (a) ER random networks of two different sizes $N = 4096$ ($\square$) and $N = 16384$ ($\circ$) and, (b) SF random networks (After [Sreenivasan et al., 2004; Sreenivasan et al., 2005]).

We make the following observations regarding the min-max path:

(i) For $r_n < p_c$, the values of r_n decrease linearly with rank n, implying that the values of r for black links are uniformly distributed between 0 and p_c, consistent with the results of Ref. [Szabó et al., 2003]. This is shown in Fig. 8.

(ii) The average number of black links, $\langle \ell_b \rangle$, along the min-max path increases linearly with the average path length ℓ_∞. This is shown in Fig. 9a.

(iii) The average number of gray links $\langle \ell_g \rangle$ along the min-max path increases logarithmically with the average path length ℓ_∞ or, equivalently, with the network size N. This is shown in Fig. 9b.
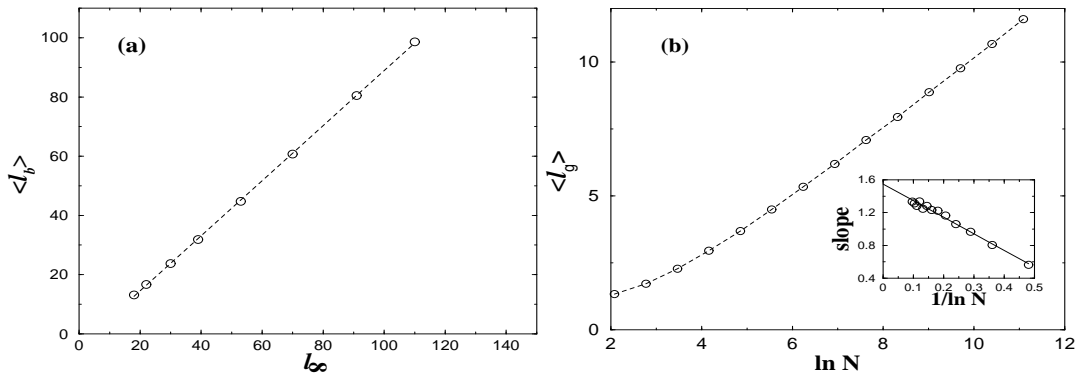

FIG. 9: (a) The average number of links $\langle \ell_b \rangle$ with random number values $r \leq p_c$ on the min-max path plotted as a function of its length ℓ_∞ for an ER network, showing that $\langle \ell_b \rangle$ grows linearly with ℓ_∞. (b) The average number of links $\langle \ell_g \rangle$ with random number values $r > p_c$ on the min-max path versus $\ln N$ for an ER network, showing that $\langle \ell_g \rangle \sim \ln N$. The inset shows the successive slopes, indicating that in the asymptotic limit $\langle \ell_g \rangle \approx 1.55 \ln N$ (After [Sreenivasan et al., 2004; Sreenivasan et al., 2005]).

The simulation results presented in Fig. 9 are for ER networks; however, we have confirmed that the observations (ii) and (iii) are also valid for SF networks with $\lambda > 3$ [Sreenivasan et al., 2004; Kalisky et. al, 2006].

Next we discuss our observations using the concept of the MST. The path on the MST between any two nodes A and B, is the optimal path between the nodes in the strong disorder limit—i.e, the min-max path.

In order to construct the MST we use the bombing algorithm (See Section II D). At the point that one cannot remove more links without disconnecting the graph, the number of

remaining black links is

$$N_b = \frac{N\langle k\rangle p_c}{2},\tag{50}$$

where $\langle k\rangle$ is the average degree of the original graph and p_c is given by [Cohen *et al.*, 2000]

$$p_c = \frac{\langle k\rangle}{\langle k^2 - k\rangle}.\tag{51}$$

The black links give rise to N_c disconnected clusters. One of these is a spanning cluster, called the *giant component* or IIC (see Section II F). The N_c clusters are linked together into a connected tree by exactly $N_c - 1$ gray links (see Fig. 10). Each of the N_c clusters is itself a tree, since a random graph can be regarded as an infinite dimensional system, and at the percolation threshold in an infinite dimensional system the clusters can be regarded as trees. Thus the N_c clusters containing N_b black links, together with $N_c - 1$ gray links form a spanning tree consisting of $N_b + N_c - 1$ links.
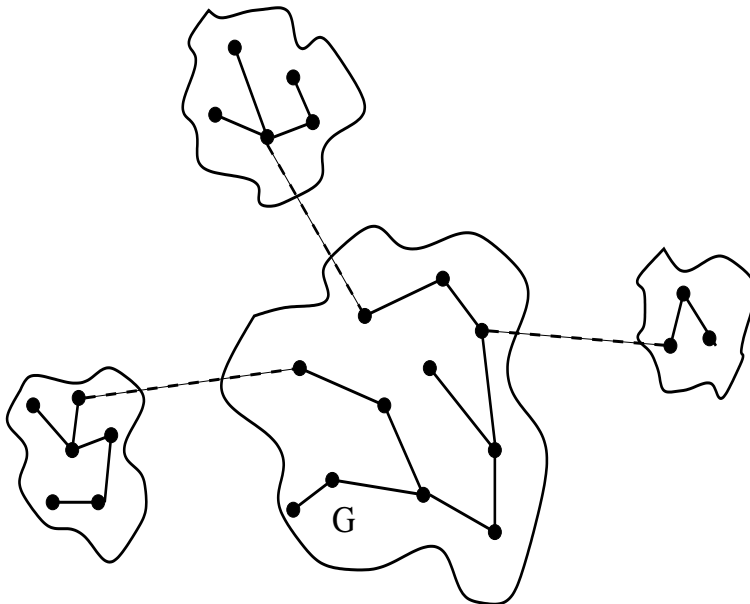

FIG. 10: Schematic representation of the structure of the minimal spanning tree, at the percolation threshold, with G being the giant component. Inside each cluster, the nodes are connected by black links to form a tree. The dotted lines represent the gray links which connect the finite clusters to form the gray tree. In this example $N_c = 4$ and the number of gray links equals $N_c - 1 = 3$ (After [Sreenivasan *et al.*, 2004; Sreenivasan *et al.*, 2005]).

Thus the MST provides *all* min-max path between any two sites on the graph. Since the

MST connects all N nodes, the number of links on this tree must be $N - 1$, so

$$N_b + N_c = N. \tag{52}$$

¿From Eq. (50) and Eq. (52) it follows that

$$N_c = N \left(1 - \frac{\langle k \rangle p_c}{2}\right). \tag{53}$$

Therefore N_c is proportional to N.

A path between two nodes on the MST consists of ℓ_b black links. Since the black links are the links that remain after removing all links with $r > p_c$, the random number values r on the black links are uniformly distributed between 0 and p_c in agreement with observation (i) and Ref. [Szabó *et al.*, 2003].

Since there are N_c clusters which include clusters of nodes connected by black links as well as isolated nodes, the MST can be described as an effective tree of N_c "super" nodes, each representing a cluster, and $N_c - 1$ gray links. We call this tree the "gray tree" (see Fig. 10). This tree is in fact a scale free tree[6] [Kalisky *et. al*, 2006] with degree exponent $\lambda_g = 2.5$ for ER networks and for scale for networks with $\lambda \geq 4$, and $\lambda_g = (2\lambda - 3)/(\lambda - 2)$ for SF networks with $3 < \lambda < 4$. If we take two nodes A and B on the original network, they will most likely lie on two distinct effective nodes of the gray tree. The number of gray links encountered on the min-max path connecting these two nodes will therefore equal the number of links separating the effective nodes on the gray tree. Hence the average number of gray links $\langle \ell_g \rangle$ encountered on the min-max path between an arbitrary pair of nodes on the network is simply the average diameter of the gray tree. Our simulation results (see Fig. 9b) indicate that

$$\langle \ell_g \rangle \sim \ln N. \tag{54}$$

Since $\langle \ell_g \rangle \sim \ln \ell_\infty \ll \ell_\infty$, the average number of black links $\langle \ell_b \rangle$ on the min-max path scales as ℓ_∞ in the limit of large ℓ_∞ in agreement with observation (2) as shown in Fig. 9a.

Next we discuss the implications of our findings for the crossover from strong to weak disorder. From observations (i) and (ii), it follows that for the portion of the path belonging to the giant component, the distribution of random values r is uniform. Hence we can approximate the sum of weights by [Kalisky *et al.*, 2005],

$$\sum_{k=1}^{\ell_b} \exp(ar_k) \approx \frac{\ell_b}{p_c} \int_0^{p_c} \exp ar \, dr = \frac{\ell_b}{ap_c} \left(\exp(ap_c) - 1\right) \equiv \exp(ar^*), \tag{55}$$

where $r^* \approx p_c + (1/a) \ln(\langle \ell_b \rangle / a p_c)$. Since $\langle \ell_b \rangle \approx \ell_\infty$,

$$r^* \approx p_c + \frac{1}{a} \ln \left(\frac{\ell_\infty}{a p_c} \right). \tag{56}$$

Thus restoring a short-cut link between two nodes on the optimal path with $p_c < r < r^*$ may drastically reduce the length of the optimal path. When $a p_c \gg \ell_\infty$, $r^* < p_c$ and such a link does not exists, if $\ell_\infty > a p_c$, the probability that such a link exist becomes positive. Hence when the min-max path is of length $\ell_\infty \approx a p_c$, the optimal path starts deviating from the min-max path. The length of the min-max path at which the deviation first occurs is precisely the crossover length $\ell^*(a)$, and therefore $\ell^*(a) \sim a p_c$. In the case of a network with an arbitrary degree distribution we can write using Eq. (51), $\ell^*(a) \sim a \frac{\langle k \rangle}{\langle k^2 - k \rangle}$.

Note that in the case of SF networks, as $\lambda \to 3^+$, p_c approaches zero and consequently $\ell^*(a) \to 0$. This suggests that for any finite value of disorder strength a, a SF network with $\lambda \leq 3$ is in the weak disorder regime. We perform numerical simulations and show that the results agree with our theoretical predictions. For the details of our simulation methods see Section II.

¿From our theoretical arguments, $\ell^*(a) \sim a$ and therefore, from Eq. (47), $W(a)$ must be a function of ℓ_∞ / a. In Fig. 11 we show the ratio $W(a)$ for different values of a plotted against $\ell_\infty / \ell^*(a) \equiv \ell_\infty / a$ for ER networks with $\langle k \rangle = 4$ and for SF networks with $\lambda = 3.5$. The excellent data collapse is consistent with the scaling relations Eq. (47). Fig. 12 shows the scaled quantities $W(a) u = \ell_{\mathrm{opt}}(a) / \ell^*(a)$ vs. $\ln u \equiv \ln(\ell_\infty / \ell^*(a)) \equiv \ln(\ell_\infty / a)$, for both ER networks with $\langle k \rangle = 4$ and for SF networks with $\lambda = 3.5$. The curves are linear at large $u \equiv \ell_\infty / \ell^*(a)$, supporting the validity of the logarithmic term in Eq. (48) for large u.

To summarize, for both ER random networks and SF networks we obtain a scaling function for the crossover from weak disorder characteristics to strong disorder characteristics. We show that the crossover occurs when the min-max path reaches a crossover length $\ell^*(a)$ and $\ell^*(a) \sim a$. Equivalently, the crossover occurs when the network size N reaches a crossover size $N^*(a)$, where $N^*(a) \sim a^3$ for ER networks and for SF networks with $\lambda \geq 4$ and $N^*(a) \sim a^{\frac{\lambda-1}{\lambda-3}}$ for SF networks with $3 < \lambda < 4$.
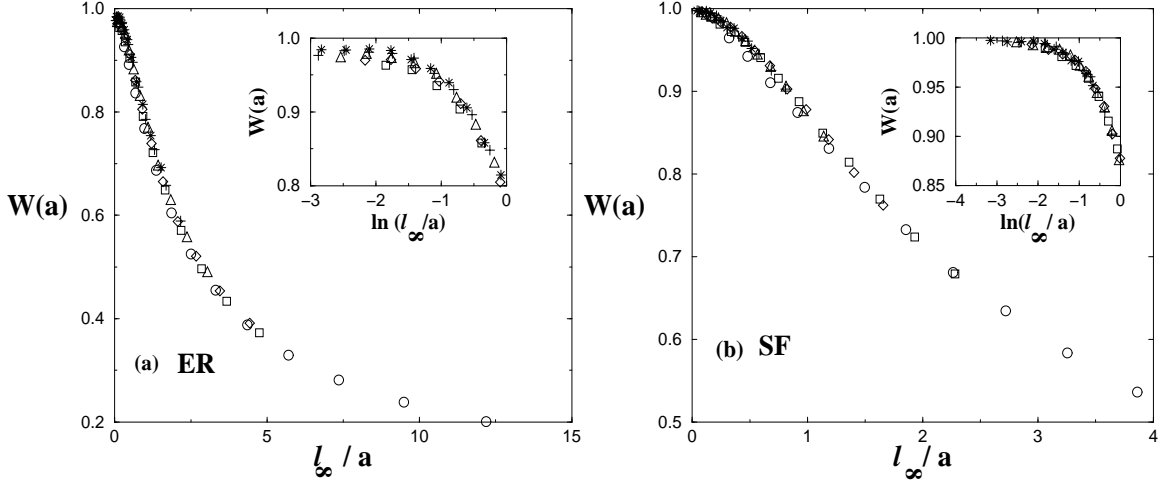
FIG. 11: Test of Eqs. (47) and (48). (a) $W(a)$ plotted as a function of ℓ_∞/a for different values of a for ER networks with $\langle k \rangle = 4$. The different symbols represent different a values: $a = 8(\circ)$, $a = 16(\square)$, $a = 22(\diamond)$, $a = 32(\triangle)$, $a = 45(+)$, and $a = 64(*)$. (b) Same for SF networks with $\lambda = 3.5$. The symbols correspond to the same values of disorder as in (a). The insets show $W(a)$ plotted against $\log(l_\infty/a)$, and indicate for $\ell_\infty \ll a$, $W(a)$ approaches a constant in agreement with Eq. (48) (After [Sreenivasan et al., 2004; Sreenivasan et al., 2005]).

B. General Disorder: Criterion for SD, WD crossovers

Until now we considered a specific form of $P(\tau) \equiv P(\tau, a) = 1/(a\tau)$ with $1 < \tau < e^a$. The question is what happens for other distributions of weights and what is the general criterion to determine which form of $P(\tau)$ can lead to strong disorder, and what is the general condition for strong or weak disorder crossover. We present analytical results [Chen et. al, 2006] for such a criterion which are supported by extensive simulations. Using this criterion we show that certain power law distributions and lognormal distributions, $P(\tau, a)$, where a is a parameter determining the broadness of the distribution, can lead to strong disorder and to a weak-strong disorder crossover [Porto et al., 1999; Braunstein et al., 2003; Sreenivasan et al., 2004]. We also show that for $P(\tau, a)$ uniform, Poisson or Gaussian, only weak disorder occurs regardless of the broadness of $P(\tau, a)$. Importantly, we find that for all $P(\tau, a)$ that possess a strong-weak disorder crossover, the distributions of the optimal path lengths display the same universal behavior.

If we express τ in terms of a random variable r uniformly distributed in $[0, 1]$, we can use the same gray and black link formalism as in the previous section. This can be achieved by
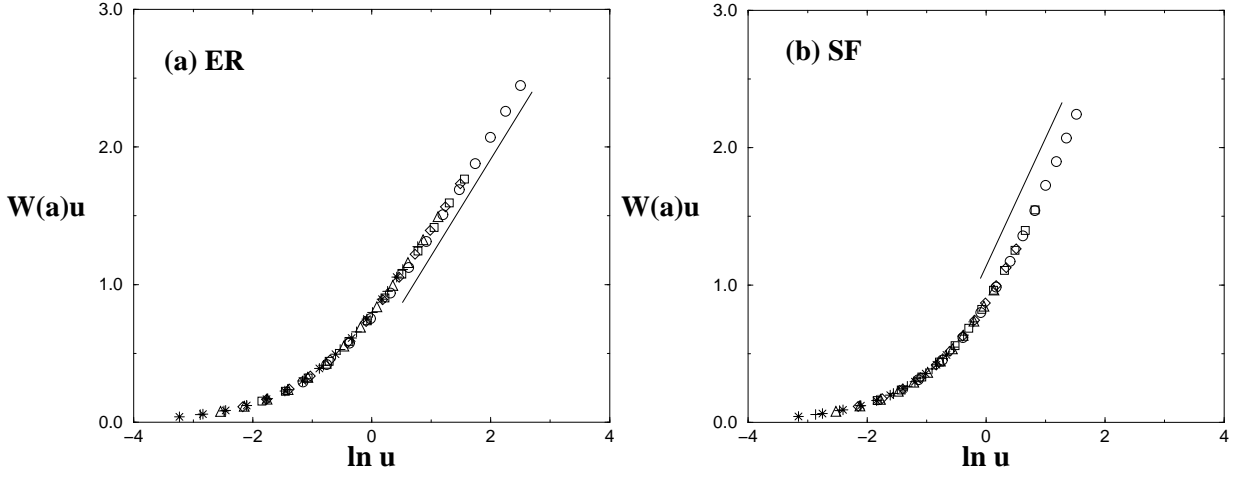
FIG. 12: (a) Plot of $W(a)u = \ell_{\text{opt}}(a)/\ell^*(a) = \ell_{\text{opt}}(a)/a$ vs $\ln u \equiv \ln(\ell_\infty/\ell^*(a)) = \ln(\ell_\infty/a)$ for ER networks with $\langle k \rangle = 4$ for different values of a. (b) Plot of $W(a)u = \ell_{\text{opt}}(a)/\ell^*(a) = \ell_{\text{opt}}(a)/a$ vs $\ln u = \ln(\ell_\infty/\ell^*(a)) = \ln(\ell_\infty/a)$ for SF networks with $\lambda = 3.5$. The values of a represented by the symbols in (a) and (b) are the same as in Fig. (8) (After [Sreenivasan *et al.*, 2004; Sreenivasan *et al.*, 2005]).

defining $r(\tau)$ by a relation:

$$r(\tau) = \int_0^\tau P(\tau', a)d\tau'. \tag{57}$$

Solving this equation with respect to τ gives us $\tau(r, a) = f(r, a)$, where $f(r, a)$ satisfies the relation

$$r = \int_0^{f(r,a)} P(\tau', a)d\tau'. \tag{58}$$

For a strong disorder regime, the sum of the weights of the black links on the IIC must be smaller than the smallest weight of the removed link $\tau_c = f(p_c, a)$:

$$\sum_{i=1}^{\ell_b} \tau_i = \sum_{i=1}^{\ell_b} f(r_i, a) < \tau_c, \tag{59}$$

where r_i are independent random variables uniformly distributed on $[0, p_c]$. As we shown above, $\ell_b \approx \ell_\infty$ so in the following we will replace ℓ_b by the average path length in the strong disorder limit, ℓ_∞. The transition to weak disorder begins when the probability that this sum is greater than τ_c becomes substantial. The investigation of this condition belongs to the realm of pure mathematics and can be answered explicitly for any functional form $f(r, a)$. This condition is satisfied when the mathematical expectation of the sum is greater

than τ_c.

$$\frac{\ell_\infty}{p_c} \int_0^{p_c} f(r,a)dr > \tau_c. \tag{60}$$

Thus the crossover to weak disorder happens if

$$\ell_\infty > A \equiv \frac{f(p_c,a)p_c}{\int_0^{p_c} f(r,a)dr} = \frac{\tau_c p_c}{\int_0^{\tau_c} \tau P(\tau,a)d\tau}, \tag{61}$$

where A plays the role of the disorder strength and τ_c satisfies the equation $p_c = \int_0^{\tau_c} P(\tau,a)d\tau$. In order for the strong disorder to exist for any network size N, the disorder strength must diverge together with the parameter a of the weight distribution $a \to \infty$. In order to determine if a network exhibits a strong disorder behavior it is useful to introduce a scaling variable

$$Z \equiv \ell_\infty/A, \tag{62}$$

so that if $Z \gg 1$ the network is in the weak disorder regime and if $Z \ll 1$, the network is in the strong disorder regime.

Note that if $f'/f > A_0$ on the entire interval $[0,1]$, then $A > A_0 p_c$. Thus another sufficient condition for a strong disorder to exist is

$$f'/f > \ell_\infty/p_c. \tag{63}$$

For the exponential disorder function $\tau = \exp(ar)$, we have $f'/f = a$ and thus Eq.(63) coincides with the condition of strong disorder $ap_c > \ell_\infty$ derived in the previous Section.

In the following, we will show how the above condition is related to the strong to weak crossover condition for the optimal path on lattices [Cieplak et $al.$, 1996; Porto et $al.$, 1999; Buldyrev et $al.$, 2006]. For the optimal path in the strong disorder limit connecting the opposite sides of the lattice of linear size L, the largest random number r_1 follows a distribution characterized by a width which scales as $L^{-1/\nu}$, where ν is the percolation connectivity length exponent [Stauffer & Aharony, 1994; Bunde & Havlin, 1996; Coniglio, 1982; Kalisky & Cohen, 2006]. The transition to weak disorder starts when the optimal path may prefer to go through a slightly larger value r_2, taken from the same distribution and thus $r_2 - r_1 \sim p_c L^{-1/\nu}$. The condition for this to happen is $[f(r_2) - f(r_1)]/f(r_1) < 1$, which is equivalent to

$$f'/f < L^{1/\nu}/p_c. \tag{64}$$

Now we will show that this condition is equivalent to (63). Percolation on Erdős-Rényi (ER) networks is equivalent to percolation on a lattice at the upper critical dimension $d_c = 6$

[Bunde & Havlin, 1996; Cohen *et al.*, 2002]. For $d = 6$, $L \sim N^{1/6}$, and $\nu = 1/2$. Thus indeed $L^{1/\nu} \sim N^{1/(d_c\nu)} \sim \ell_\infty$ [Braunstein *et al.*, 2003].

Following similar arguments for a scale-free network with degree distribution $P(k) \sim k^{-\lambda}$ and $3 < \lambda < 4$, we can replace $L^{-1/\nu}$ by $N^{-(\lambda-3)/(\lambda-1)}$ since $d_c = 2(\lambda - 1)/(\lambda - 3)$ [Cohen *et al.*, 2002]. Thus, due to Eq. (38) $L^{1/\nu} \sim \ell_\infty$ and we can introduce the analogous scaling parameter Z for lattices:

$$Z = \frac{L^{1/\nu}}{p_c f'/f}. \tag{65}$$

Next we calculate A for several specific weight distributions $P(\tau)$ [Chen *et. al*, 2006]. We begin with the well-studied exponential disorder function $f(x) = e^{ar}$, where r is a random number between 0 and 1 [Strelniker *et al.*, 2004; Cieplak *et al.*, 1996]. From Eq. (58) follows that $P(\tau, a) = 1/(a\tau)$, where $\tau \in [1, e^a]$. Using Eq. (61) we have

$$A = ap_c\tau_c/(\tau_c - 1) \sim ap_c; \tag{66}$$

For fixed A, but different a and p_c, we expect to obtain the same optimal path behavior. Indeed, this has been shown to be valid [Wu *et al.*, 2005; Strelniker *et al.*, 2004; Kalisky *et al.*, 2005; Chen *et. al*, 2006].

Next we study A for the disorder function $f(r, a) = r^a$, with r between 0 and 1 where $a > 0$ [Hansen & Kertész, 2004]. For this case the disorder distribution is a power law $P(\tau, a) = a^{-1}\tau^{1/a-1}$. Following Eq. (61) we obtain

$$A = a + 1 \sim a. \tag{67}$$

Note that here a plays a similar role as a in Eq. (66), but now A is independent of p_c, which means that networks with different p_c, such as ER networks with different average degree $< k >= 1/p_c$, yield the same optimal path behavior.

For the power law distribution with negative exponent $f(r) = (1 - r)^{-a}$ $(a > 0)$, we have $P(\tau, a) = a^{-1}\tau^{-1-1/a}$ and

$$A = \frac{(a - 1)p_c(1 - p_c)^{-a}}{(1 - p_c)^{1-a} - 1} \sim \frac{ap_c}{1 - p_c}. \tag{68}$$

We further generalize the power law distribution with the disorder function $f(r, a) = r^a$ by introducing the parameter $0 \le \Delta \le 1$ which is defined as the lower bound of the uniformly distributed random number r, i.e., $1 - \Delta \le r \le 1$ [Hansen & Kertész, 2004]. Under this

40

condition, the distribution becomes

$$P(\tau, a) = \frac{\tau^{1/a-1}}{|a|\Delta} \qquad \tau \in [(1-\Delta)^a, 1].$$ (69)

Again using Eq. (61), we obtain

$$A = \frac{ap_c\Delta}{p_c\Delta + 1 - \Delta}.$$ (70)

Table VI B shows the results of similar analysis for the lognormal, Gaussian, uniform and exponential distributions $P(\tau, a)$. From Table VI B, we see that for exponential function, power law and lognormal distributions, A is proportional to a and thus can become large. However for uniform, Gaussian and exponential distributions, A is limited to a value of order 1, so $Z \gg 1$ for large N and the optimal path is always in the weak disorder regime. Note that for these distributions, A is independent of a.

In general, one can prove that $A \to \infty$ for a given distribution $P(\tau, a)$ as $a \to \infty$ if there exist a normalization function $c(a)$ and a cutoff function $\tau(a)$ such that for $\forall \epsilon > 0, \forall E > 0$, $\exists M > 0$ such that for $a > M$ and $\tau \in [\tau(a), \tau(a)E]$, $|\tau P(\tau, a)c(a) - 1| < \epsilon$. We will call such functions $P(\tau, a)$ "quasi-$1/\tau$" distributions because they behave as $1/\tau$ in a wide range of τ. Obviously that exponential, power-law and lognormal distributions are quasi-$1/\tau$ functions, so for them, for large enough a we can observe a strong disorder.

To test the validity of our theory, we perform simulations of optimal paths in $2d$ square lattices and ER networks. Random weights from different disorder functions were assigned to the bonds. For an $L \times L$ square lattice, we calculate the average length ℓ_{opt} of the optimal path from one lattice edge to the opposite. For an ER network of N nodes, we calculate ℓ_{opt} between two randomly selected nodes.

Simulations for optimal paths on ER networks are shown in Fig. 13. Here we use the bombing algorithm (See Section II D) to determine the path length ℓ_∞ in the strong disorder limit, which is related to N by $\ell_\infty \sim N^{\nu_{opt}} = N^{1/3}$ [Braunstein et al., 2003] (See Section IV). We see that for all disorder distributions studied, ℓ_{opt} scales in the same universal way with $Z \equiv \ell_\infty/A$. For $Z \gg 1$, ℓ_{opt}/A is linear with $\log(\ell_\infty/A)$ as expected (Fig. 3a). For small $Z = \ell_\infty/A$ (Fig. 13 b), $\ell_{opt} \propto \ell_\infty \sim N^{1/3}$, which is the strong disorder behavior [Braunstein et al., 2003]. Thus, we see that when N increases, a crossover from strong to weak disorder occurs in the scaled optimal paths ℓ_{opt}/A vs. Z. Again, the collapse of all curves for different disorder distributions for ER networks supports the general condition of Eq. (62).

41

Name	Function	Distribution	Domain	A
Inverse	e^{ax}	$\frac{1}{a\tau}$	$\tau \in [1, e^a]$	ap_c
Power Law	x^a	$\frac{\tau^{1/a-1}}{a}$	$\tau \in (0,1]$	a
Power Law	$(1-x)^a$	$\frac{1}{a}\tau^{1+1/a}$	$\tau \in [1,\infty]$	$a\frac{p_c}{1-p_c}$
Power Law	x^a	$\frac{\tau^{1/a-1}}{|a|\Delta}$	$\tau \in [(1-\Delta)^a, 1]$	$a\frac{p_c\Delta}{1-(1-p_c)\Delta}$
Lognormal	$e^{\sqrt{2}a\mathrm{erf}^{-1}(2x-1)}$	$\frac{e^{-(\ln\tau)^2/2a^2}}{\tau a\sqrt{2\pi}}$	$\tau \in (0,\infty)$	$a\frac{\sqrt{2\pi}p_c}{e^{-[\mathrm{erf}^{-1}(2p_c-1)]^2}}$
Uniform	ax	$1/a$	$\tau \in [0,a]$	2
Gaussian	$\sqrt{2}a\mathrm{erf}^{-1}(x)$	$\frac{2e^{-\tau^2/(2a^2)}}{a\sqrt{2\pi}}$	$\tau \in [0,\infty)$	$\frac{\sqrt{2\pi}p_c\mathrm{erf}^{-1}}{1-e^{-[\mathrm{erf}^{-1}(p_c)]^2}}$
Exponential	$-a\ln(1-x)$	$\frac{e^{-\tau/a}}{a}$	$\tau \in [0,\infty)$	$\frac{-p_c\ln(1-p_c)}{p_c+(1-p_c)\ln(1-p_c)}$

TABLE I: Parameters controlling the optimal paths on networks for various distributions of disorder (After [Chen *et. al*, 2006])
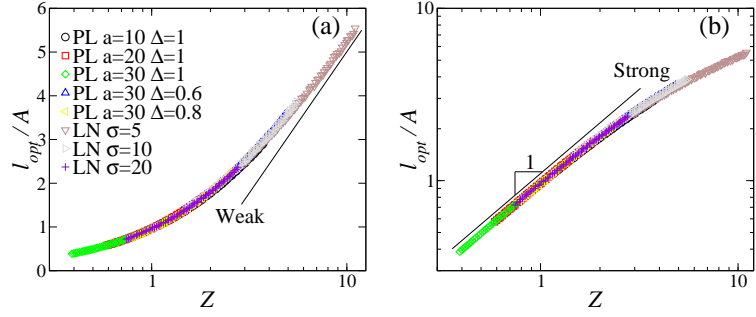
,

FIG. 13: The function ℓ_{opt}/A for ER networks after scaling, where (a) is a linear-log plot and (b) is a log-log plot. Distributions used are power law x^a with $10 \leq a \leq 30$ where $0 \leq x < 1$, x^a with $a = 30$ and the range of $\Delta < x \leq 1$ with $\Delta = 0.6$ or 0.8, and lognormal distribution with $10 \leq a \leq 30$. The straight line in (a) indicates weak disorder and the straight line in (b) indicates strong disorder (After [Chen *et. al*, 2006]).

Next we use Eq. (62) to analyze the other types of disorder given in Table VI B that do not have strong disorder behavior. For a uniform distribution, $P(\tau) = 1/a$ and we obtain $A = 1$. The parameter a cancels, so $Z = L^{1/\nu}$ for lattices, and $Z = N^{1/3}$ for ER networks. Hence for any value of a, $Z << 1$, and strong disorder behavior cannot occur for a uniform
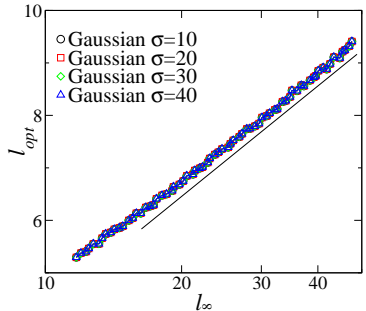
42

distribution.

FIG. 14: The optimal path for Gaussian distribution of weights for ER networks. Note that these curves would collapse after scaling to the curves in Fig. 13 in the weak disorder tail of large Z^{-1} (After [Chen $et.$ al, 2006]).

Next we analyze the Gaussian distribution. We assume that all the weights τ_j are positive and thus we consider only the positive regime of the distribution. Using Eq. (61) we obtain

$$A = \frac{\sqrt{2\pi}p_c\mathrm{erf}^{-1}}{1 - e^{-[\mathrm{erf}^{-1}(p_c)]^2}}. \tag{71}$$

The disorder is controlled solely by p_c which is related only to the type of network, and A cannot take on large values. Thus, also for the Gaussian $P(\tau, a)$, all optimal paths are in the weak disorder regime. Similar considerations lead to the same conclusion for the exponential distribution where $A = \frac{-p_c\ln(1-p_c)}{p_c+(1-p_c)\ln(1-p_c)}$. Simulation results for the Gaussian distribution shown in Fig. 14 display only weak disorder (i.e. no weak-strong disorder crossover), thus supporting the above conclusions.

To summarize, in this section we presented a criterion for the inverse disorder strength Z on the optimal path in weighted networks for general distributions $P(\tau, a)$. We show an analytical expression, Eq. (61), which fully characterizes the behavior of the optimal path. Simulation of several distributions support these analytical predictions. It is plausible that the criterion of Eq. (61) is valid also for other physical properties in weighted networks — such as conductivity and flow in random resistor networks — due to a recently-found close relation between the optimal path and flow [Strelniker et $al.$, 2004; Wu et $al.$, 2005].

VII.   SCALING OF OPTIMAL-PATH-LENGTHS DISTRIBUTION WITH FINITE DISORDER IN COMPLEX NETWORKS

In this chapter we present further support [Kalisky *et al.*, 2005] for the general analytical results presented in section VIB. The question is how the different optimal paths in a network are distributed? The distribution of the optimal path lengths is especially important in communication networks, in which the overall network performance depends on the different path lengths between all nodes of the network, and not only the average. Ref. [Sreenivasan *et al.*, 2004] studied the probability distribution $P(\ell_{\text{opt}})$ of optimal path lengths in an ER network in the SD limit. The scaled curve for $P(\ell_{\text{opt}})$ for different network sizes is shown in Fig. 15 in a log-log plot. We find that similarly to the behavior of self avoiding walks [de Gennes, 1979] there are two regimes in this distribution, the first one being a power law $P(\ell_{\text{opt}}) \sim (\ell_{\text{opt}})^g$ which is evident from the figure, with $g \approx 2$. The second regime is an exponential $P(\ell_{\text{opt}}) \sim e^{-C\ell_{\text{opt}}^\delta}$ where C is a constant and δ is around 2. This leads us to the conjecture that the distribution may have a Maxwellian functional form:

$$P(\ell_{\text{opt}}) = \frac{4\ell_{\text{opt}}^2 e^{-(\ell_{\text{opt}}/l_o)^2}}{\sqrt{\pi} l_o^3}, \tag{72}$$

Where $\ell_o = \sqrt{\pi}\langle\ell_{\text{opt}}\rangle/2$ is the most probable value of ℓ_{opt}. The solid line in the figure is the plot of this function and as seen it agrees with our numerical results.

The exponents g and δ can be obtained from the following heuristic arguments. The right tail of the distribution $P(\ell_{\text{opt}})$ is determined by the distribution of the IIC size in the network of N nodes. At percolation threshold (Sec. VI), N nodes are divided into $N/2$ clusters, obeying the power law distribution. However, the sum of all the cluster sizes is equal to N, thus the distribution of the largest cluster sizes must have a finite size exponential cutoff $P(S) \sim \exp(-CS)$, as for the distribution of the segments of an interval divided by random partitions. Since $S \sim \ell_{\text{opt}}^{d_\ell}$, we have $\delta = d_\ell$.

To find the left tail distribution, we use the concept of MST. The chemical diameter of the MST is ℓ_{opt} while its mass is $N \sim \ell_{\text{opt}}^{1/\nu_{\text{opt}}}$. Due to self-similarity of the MST the number of nodes $n(\ell)$ within a chemical distance ℓ also scales as $n(\ell) \sim \ell^{1/\nu_{\text{opt}}}$. Thus the probability density of the of the optimal path for small values of ℓ scales as $dn(\ell)/d\ell = \ell^{1/\nu_{\text{opt}}-1}$. Hence $g = 1/\nu_{\text{opt}} - 1$. We expect that our conjecture is valid also for SF networks. Using Eqs. (37)

44

and (38) we have:

$$\delta = d_\ell = \begin{cases} 2, & \lambda > 4, \quad \text{ER} \\ (\lambda - 2)/(\lambda - 3), & 3 < \lambda \leq 4 \end{cases}, \tag{73}$$

and

$$g = \begin{cases} 2, & \lambda > 4, \quad \text{ER} \\ 2/(\lambda - 3), & 3 < \lambda \leq 4 \end{cases}. \tag{74}$$
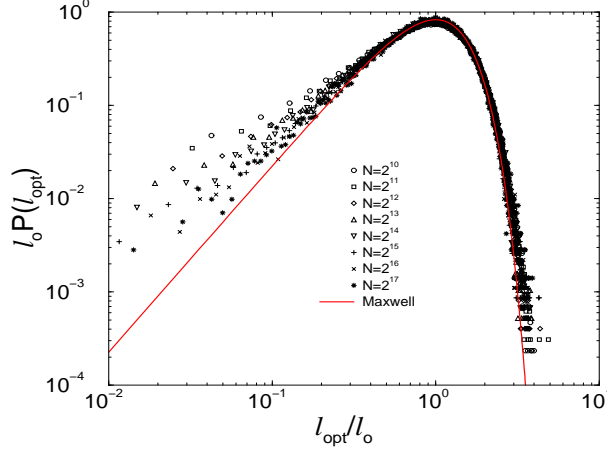

FIG. 15: Scaled curve for the probability distribution $P(\ell_{\text{opt}})$ of optimal path lengths for network sizes $N = 1024, 2048, 4096, 8192, 16384, 32768, 65536$. The gray curve represents Maxwellian fit given by Eq. (72) (After [Buldyrev *et al.*, 2003]).

A recent work has studied the distribution form of shortest path lengths on minimum spanning trees [Braunstein *et al.*, 2004], which corresponds to optimal paths on networks with large variation in link weights $(a \to \infty)$.

Using the scaling derived in Sect. VI, more precisely:

$$\ell(a) \sim \ell_\infty F\left(\frac{\ell_\infty}{ap_c}\right), \tag{75}$$

where p_c is the percolation threshold and $\ell_\infty \sim N^{\nu_{opt}}$ is the optimal path length for strong disorder $(a \to \infty)$. For Erdős-Rényi (ER) graphs $\nu_{opt} = 1/3$. We generalize these results and suggest that the distribution of the optimal path lengths has the following scaling form:

$$P(\ell_{\text{opt}}, N, a) \sim \frac{1}{\ell_\infty} G\left(\frac{\ell_{\text{opt}}}{\ell_\infty}, \frac{1}{p_c}\frac{\ell_\infty}{a}\right). \tag{76}$$

The parameter $Z \equiv \frac{1}{p_c}\frac{\ell_\infty}{a}$, which is equivalent to Z in Eq. (62), determines the functional form of the distribution. Relation (76) is supported by simulations [Kalisky *et al.*, 2005] for

both ER and SF graphs, including SF graphs with $2 < \lambda < 3$, for which $p_c \to 0$ with system size N [Cohen *et al.*, 2000].

We simulate ER graphs with weights on the links for different values of graph size N, control parameter a, and average degree $\langle k \rangle$ (which determines $p_c = 1/\langle k \rangle$). We then generate the shortest path tree (SPT) using Dijkstra's algorithm (See Section II B) from some randomly chosen root node. Next, we calculate the probability distribution function of the optimal path lengths for all nodes in the graph [Kalisky *et al.*, 2005].

In Fig. 16 we plot $\ell_\infty P(\ell_{\text{opt}}, N, a)$ vs. $\ell_{\text{opt}}/\ell_\infty$ for different values of N, a, and $\langle k \rangle$. A collapse of the curves is seen for all graphs with the same value of $Z = \frac{1}{p_c} \frac{\ell_\infty}{a}$.

Figure 17 shows similar plots for SF graphs – with a degree distribution of the form $P(k) \sim k^{-\lambda}$ and with a minimal degree m. Scale-free graphs were generated according to the "configuration model" or Molloy Reed algorithm (See Section IIA) [Molloy & Reed, 1998] [7]. A collapse is obtained for different values of N, a, λ and m, with $\lambda > 3$ and for the same values of Z.

Next, we study SF networks with $2 < \lambda < 3$. In this regime the second moment of the degree distribution $\langle k^2 \rangle$ diverges, leading to several anomalous properties [Cohen *et al.*, 2000; Cohen & Havlin, 2003; Callaway *et al.*, 2000]. For example: the percolation threshold approaches zero with system size according to Eq. (25): $p_c \sim N^{-\frac{3-\lambda}{\lambda-1}} \to 0$, and the optimal path length ℓ_∞ in SD was found numerically to scale logarithmically with N compared to polynomially, found in $\lambda > 3$ [Braunstein *et al.*, 2003]. Nevertheless, it seems from Fig. 18 that the optimal paths probability distribution for SF networks with $2 < \lambda < 3$ exhibits similar collapse for different values of N and a for the same Z (although its functional form is different compared to the $\lambda > 3$ case) [Kalisky *et al.*, 2005].

We present evidence that the optimal path is related to percolation [Sreenivasan *et al.*, 2004]. The numerical results suggest that for a finite disorder parameter a, the optimal path (on average) follows the percolation cluster in the network (i.e., links with weight below p_c) up to a typical "characteristic length" $\xi = ap_c$, before deviating and making a "shortcut" (i.e. crossing a link with weight above p_c). For length scales below ξ the optimal path behaves as in strong disorder and its length is relatively long. The shortcuts have an effect of shortening the optimal path length from a polynomial to logarithmic form according to the universal function $F(u)$ (Eq. (75)). Thus, the optimal path for finite a can be viewed as consisting of "blobs" of size ξ in which strong disorder persists. These blobs are
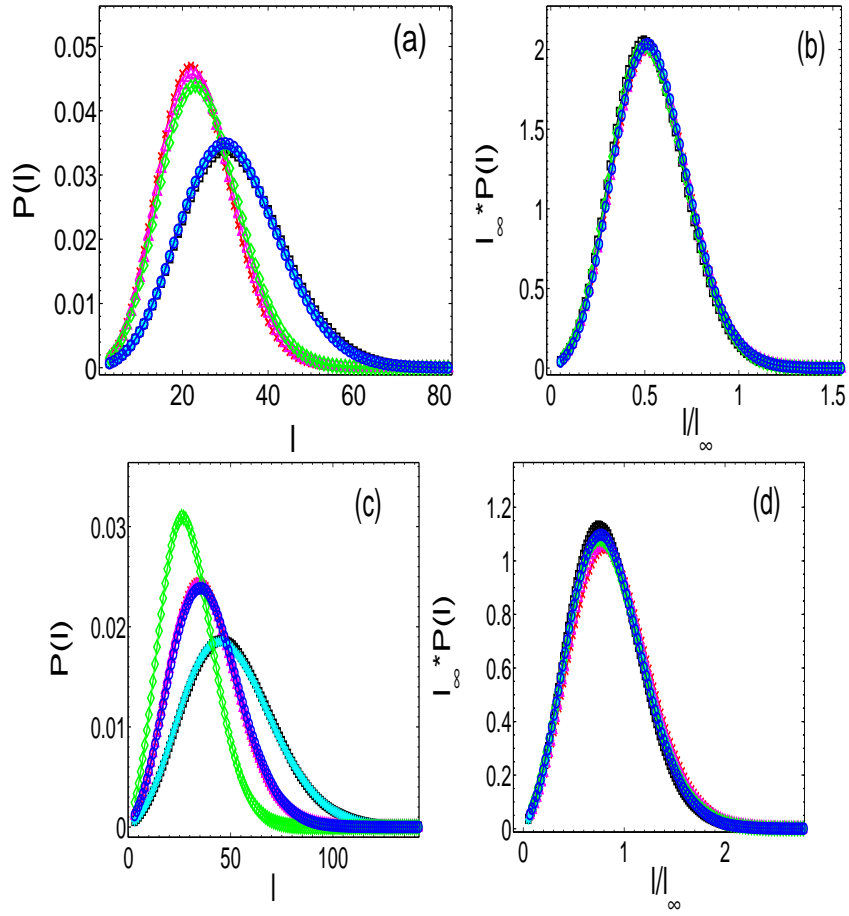
46

FIG. 16: Optimal path lengths distribution, $P(\ell_{\text{opt}})$, for ER networks with (a,b) $Z \equiv \frac{1}{p_c} \frac{\ell_\infty}{a} = 10$ and (c,d) $Z = 3$. (a) and (c) represent the unscaled distributions for $Z = 10$ and $Z = 3$ respectively, while (b) and (d) are the scaled distribution. Different symbols represent networks with different characteristics such as size $N = 2000, 4000, 8000$ (which determines $\ell_\infty \sim N^{1/3}$), average degree $\langle k \rangle = 3, 5, 8$ (which determines $p_c = 1/\langle k \rangle$), and disorder strength $a = \ell_\infty/(p_c Z)$ Results were averaged over 1500 realizations (After [Kalisky et $al.$, 2005]).

interconnected by shortcuts, which result in the total path being in weak disorder.

We next present direct simulations supporting this argument [Kalisky et $al.$, 2005]. We calculate the optimal path length $\ell(a)$ inside a single network of size N, for a given a, and find (Fig. 19) that it scales differently below and above the characteristic length $\xi = a p_c$. For each node in the graph we find ℓ_{min}, which is the number of links ("hopcounts") along the shortest path from the root to this node $without$ $regarding$ the $weight$ of the $link$.

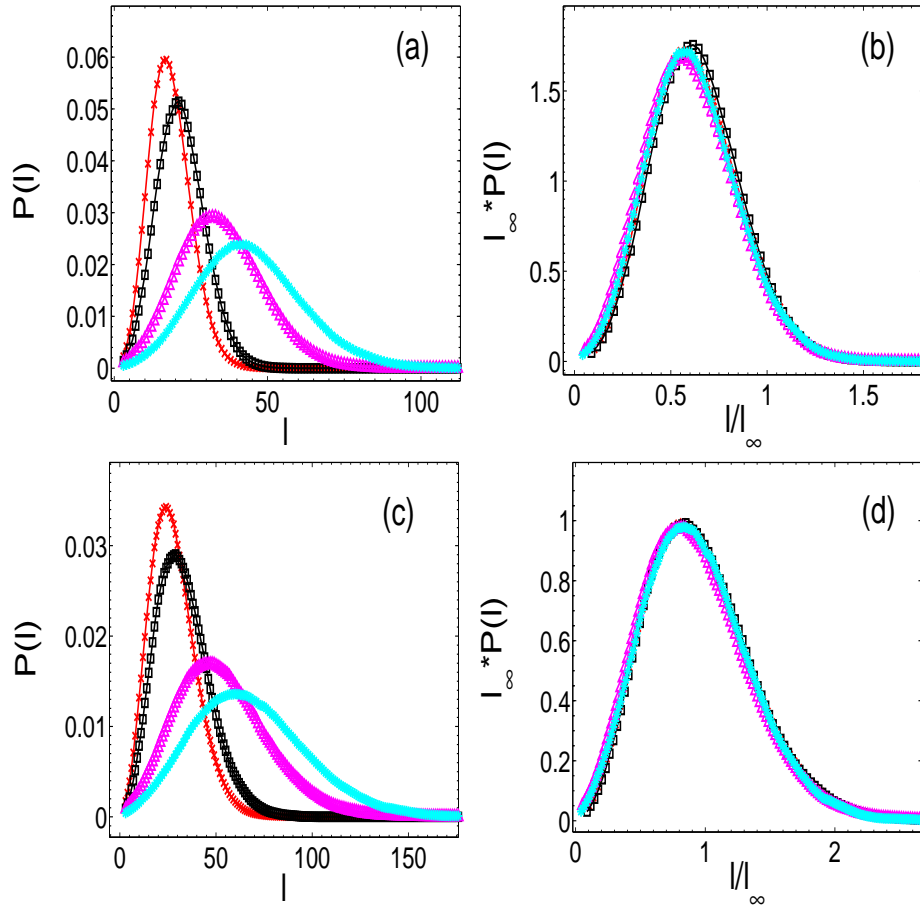In Fig. 19 we plot the length of the optimal path $\ell(a)$, averaged over all nodes with the

FIG. 17: Optimal path lengths distribution, $P(l)$, for SF networks with (a,b) $Z \equiv \frac{1}{p_c} \frac{\ell_\infty}{a} = 10$ and (c,d) $Z = 2$. (a) and (c) represent the unscaled distributions for $Z = 10$ and $Z = 2$ respectively, while (b) and (d) are the scaled distribution. Different symbols represent networks with different characteristics such as size $N = 4000, 8000$ (which determines $\ell_\infty \sim N^{\nu_{opt}}$), $\lambda = 3.5, 5$ and $m = 2$ (which determine p_c), and disorder strength $a = \ell_\infty/(p_c Z)$. Results were averaged over 250 realizations (After [Kalisky *et al.*, 2005]).

same value of ℓ_{min} for different values of a. The figure strongly suggests that $l(a) \sim \exp(\ell_{min})$ for length scales below the characteristic length $\xi = a p_c$ (see the linear regime in Fig. 19b), while for large length scales $\ell(a) \sim \ell_{min}$.

For length scales smaller than ξ we have $\ell_{opt} = A N^{1/3}$ and $\ell_{min} = B \ln N$, where A and B are constants. Thus $N = \exp(\ell_{min}/B)$ and $\ell_{opt} = A \exp(l_{min}/3B)$. Consequently, we expect that: $\frac{\ell_{opt}}{\xi} = \frac{A \exp(\ell_{min}/3B)}{\xi} = A \exp[(l_{min} - 3B \ln \xi)/3B]$. We find the best scaling in Fig. 19 for $B = \frac{2}{3 \ln \langle k \rangle}$.
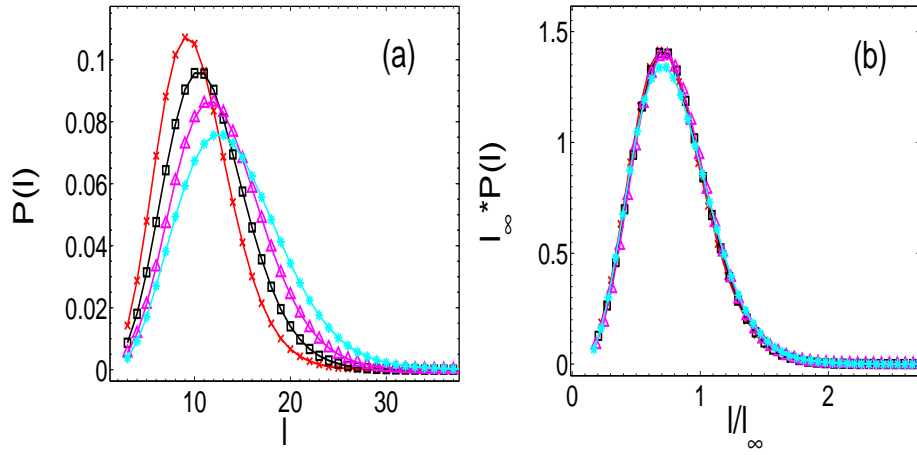
FIG. 18: Optimal path lengths distribution function for SF graphs with $\lambda = 2.5$, $m = 2$ and with $Z \equiv \frac{1}{p_c}\frac{\ell_\infty}{a} = 10$. (a) represents the unscaled distribution for $Z = 10$ while (b) shows the scaled distribution. Different symbols represent graphs with different characteristics such as size $N = 2000, 4000, 8000, 1600$ (which determines $\ell_\infty \sim \log(N)$ and $p_c \sim N^{-1/3}$), and disorder strength $a = \ell_\infty/(p_c Z)$. Results were averaged over 1500 realizations (After [Kalisky et al., 2005]).

This is consistent with our hypothesis that below the characteristic length ($\xi = ap_c$) $\ell_{min} \sim \log N$ and $l(a) \sim N^{1/3}$, while $\ell_{min} \sim \log N$ and $l(a) \sim \log N$ above.

In order to better understand why the distributions of ℓ_{opt} depend on Z according to Eq. (76), we suggest the following argument. The optimal path for $a \to \infty$, was shown to be proportional to $N^{1/3}$ for ER graphs and $N^{(\lambda-3)/(\lambda-1)}$ for SF graphs with $3 < \lambda < 4$ [Braunstein et al., 2003]. For finite a the number of shortcuts, or number of blobs, is $Z = \frac{\ell_\infty}{\xi} = \frac{\ell_\infty}{ap_c}$. The deviation of the optimal path length for finite a from the case of $a \to \infty$ is a function of the number of shortcuts. These results explain why the parameter $Z \equiv \frac{\ell_\infty}{ap_c}$ determines the functional form of the distribution function of the optimal paths (see also section VIB) .

To summarize, we have shown that the optimal path length distribution in weighted random graphs has a universal scaling form according to Eq. (76). We explain this behavior and demonstrate the transition between polynomial and logarithmic behavior of the average optimal path in a single graph. Our results are consistent with results found for finite dimensional systems [Porto et al., 1999; Wu et al., 2005; Strelniker et al., 2004]: In finite dimension the parameter controlling the transition is $Z = \frac{L^{1/\nu}}{ap_c}$, where L is the system length
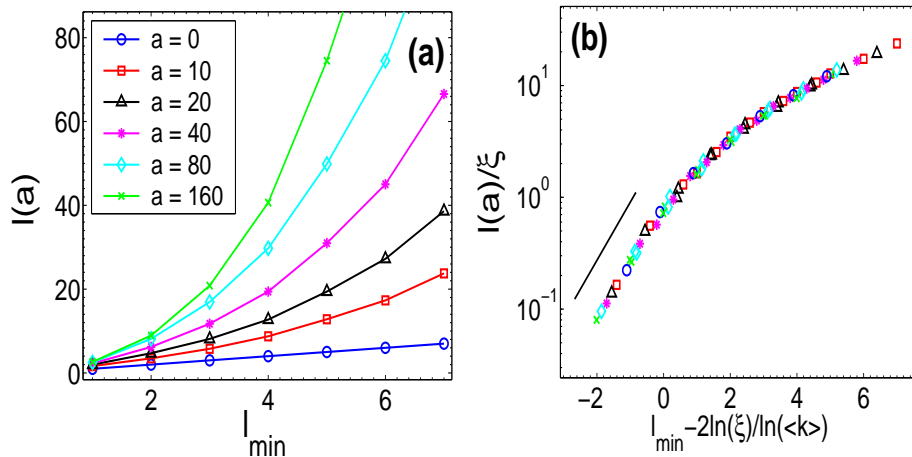
FIG. 19: Transition between different scaling regimes for the optimal path length $l(a)$ inside an ER graph with $N = 128,000$ nodes and $\langle k \rangle = 10$. (a) shows the unscaled and (b) shows the scaled length of the optimal path $l(a)$ averaged over all nodes with same value of ℓ_{min}. Different symbols represent different values of the disorder strength a. for length scales $\ell(a)$ smaller than the "characteristic length", $\xi = ap_c$, $l(a)$ grows exponentially relative to the shortest hopcount path ℓ_{min} (see solid line). This is consistent with $l(a) \sim N^{1/3}$ and $\ell_{min} \sim \log N$ inside the range of size $\xi = ap_c$. For length scales above ξ both quantities scale as $\log N$. (After [Kalisky *et al.*, 2005]).

and ν is the correlation length critical exponent as in Eq.(65). This is because only the "red bonds" - bonds that if cut would disconnect the percolation cluster [Stanley, 1977, Coniglio, 1982] - control the transition (see also section VIB).

VIII. SCALE-FREE NETWORKS EMERGING FROM WEIGHTED RANDOM GRAPHS

In this section we introduce a simple process that generates random scale-free networks with $\lambda = 2.5$ from weighted Erdös-Rényi graphs [Kalisky *et. al*, 2006]. We further show that the minimum spanning tree (MST) on an Erdös-Rényi graph is related to this network, and is composed of percolation clusters, which we regard as "super nodes", interconnected by a scale-free tree. We will see that due to optimization this scale-free tree is dominated by links having high weights — significantly higher than the percolation threshold p_c. Hence, the MST naturally distinguishes between links below and above the percolation threshold,

leading to a scale-free "supernode network". Our results may explain the origin of scale-free degree distribution in some real world networks.

Consider an Erdös-Rényi (ER) graph with N nodes and an average degree $\langle k \rangle$, thus having a total of $N\langle k \rangle/2$ links. To each link we assign a weight chosen randomly and uniformly from the range $[0,1]$. We define black links to be those links with weights below a threshold $p_c = 1/\langle k \rangle$. Two nodes belong to the same cluster if they are connected by black links [Fig. 20(a)].

¿From Section VI follows that the number of clusters of s nodes scales as a power law, $n_s \sim s^{-\tau}$, with $\tau = 2.5$ for ER networks. Next, we merge all nodes inside each cluster into a single "supernode". We define a new "supernode network" [Fig. 20(b)] of N_{sn} supernodes [Sreenivasan et $al.$, 2004]. The links between two supernodes [see Figs. 20(a) and 20(b)] have weights $larger$ than p_c. The degree distribution $P(k)$ of the supernode network can be obtained as follows. Every node in a supernode has the same (finite) probability to be connected to a node outside the supernode. Thus, we assume that the degree k of each supernode is proportional to the cluster size s, which obeys $n_s \sim s^{-2.5}$. Hence $P(k) \sim k^{-\lambda}$, with $\lambda = 2.5$, as supported by simulations shown in Fig. 21. Furthermore, we also see that if the threshold for obtaining the clusters which are merged into supernodes is changed slightly, the degree distribution still remains scale free with $\lambda = 2.5$, but with an exponential cutoff. This is an indication of the fact that there are still supernodes of high degree which are connected to many other (small) supernodes by links with weights significantly higher than p_c; if this was not the case, a small change in the threshold would cause many clusters to merge and destroy the power law in the supernode network degree distribution.

We next show that the MST on an ER graph is related to the supernode network, and therefore also exhibits scale-free properties. In the MST each path between two sites on the MST is the optimal path in the "strong disorder" limit [Cieplak et $al.$, 1996; Dobrin & Duxbury, 2001], meaning that along this path the maximum $barrier$ (weight) is the smallest possible [Dobrin & Duxbury, 2001; Braunstein et $al.$, 2003; Sreenivasan et $al.$, 2004].

Here we use the bombing algorithm (See Section IID). If the removal of a link disconnects the graph, we restore the link and mark it "gray" ; otherwise the link [shown dotted in Fig. 20(a)] is removed. The links that are not bombed are marked as "black". In the bombing algorithm, only links that close a loop can be removed. Because below criticality loops are negligible [Erdős & Rényi, 1959; Albert & Barabási, 2002] for ER networks ($d \to \infty$),

(a) Original Network

(c) MST of original Network

Black links
---- Gray links

(b) Supernode network
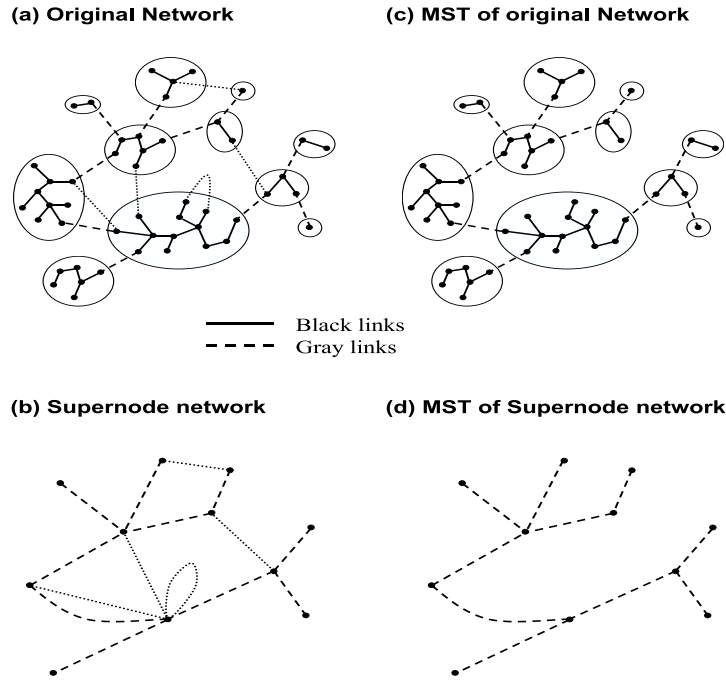
(d) MST of Supernode network

FIG. 20: Sketch of the "supernode network". (a) The original ER network, partitioned into percolation clusters whose sizes s are power-law distributed, with $n_s \sim s^{-\tau}$ where $\tau = 2.5$ for ER graphs. The "black" links are the links with weights below p_c, the "dotted" links are the links that are removed by the bombing algorithm, and the "gray" links are the links whose removal will disconnect the network (and therefore are not removed even though their weight is above p_c). (b) The "supernode network": the nodes are the clusters in the original network and the links are the links connecting nodes in different clusters (i.e., "dotted" and "gray" links). The supernode network is scale-free with $P(k) \sim k^{-\lambda}$ and $\lambda = 2.5$. Notice the existence of self loops and of double connections between the same two supernodes. (c) The minimum spanning tree (MST), composed of black and gray links only. (d) The MST of the supernode network ("gray tree"), which is obtained by bombing the supernode network (thereby removing the "dotted" links), or equivalently, by merging the clusters in the MST to supernodes. The gray tree is scale-free, with $\lambda = 2.5$ (After [Kalisky *et. al*, 2006]).

bombing does not modify the percolation clusters — where the links are black and have weights below p_c. Thus, bombing modifies only links *outside* the clusters, so actually it is only the links of the *supernode network* that are bombed. Hence the MST resulting from
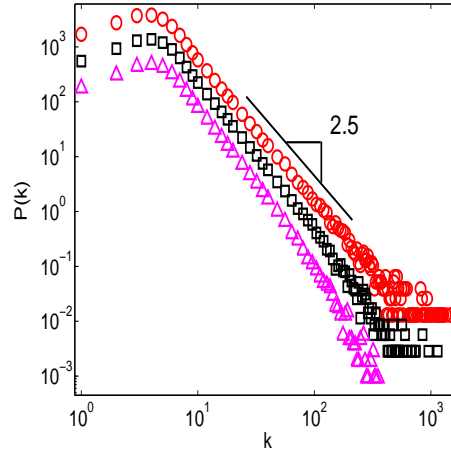
FIG. 21: The degree distribution of the supernode network of Fig. 1(b), where the supernodes are the percolation clusters, and the links are the links with weights larger than p_c (○). The distribution exhibits a scale-free tail with $\lambda \approx 2.5$. If we choose a threshold less than p_c, we obtain the same power law degree distribution with an exponential cutoff. The different symbols represent slightly different threshold values: $p_c - 0.03$ (□) and $p_c - 0.05$ (△). The original ER network has $N = 50,000$ and $\langle k \rangle = 5$. Note that for $k \approx \langle k \rangle$ the degree distribution has a maximum (After [Kalisky *et. al*, 2006]).

bombing is composed of percolation clusters (composed of black links) and connected by gray links [Fig. 20(c)].

¿From the MST of Fig. 20(c) we now generate a new tree, the MST of the supernode network, which we call the "gray tree", whose nodes are the supernodes and whose links are the gray links connecting them [see Fig. 20(d)]. Note that bombing the original ER network to obtain the MST of Fig. 20(c) is equivalent to bombing the supernode network of Fig. 20(b) to obtain the gray tree, because the links inside the clusters are not bombed. We find [Fig 22(a)] that the gray tree has also a scale-free degree distribution $P(k)$, with $\lambda = 2.5$—the same as the supernode network.[8] We also find [Fig. 22(b)] the average path length ℓ_{gray} scales as $\ell_{\text{gray}} \sim \log N_{\text{sn}} \sim \log N$ [Sreenivasan *et al.*, 2004].[9] Note that even though the gray tree is scale-free, it is not ultra-small [Cohen & Havlin, 2003], since the length does not scale as $\log \log N$.

Next we show that the bombing optimization, which leads to the MST, yields a significant separation between the weights of the links inside the supernodes and the links connecting
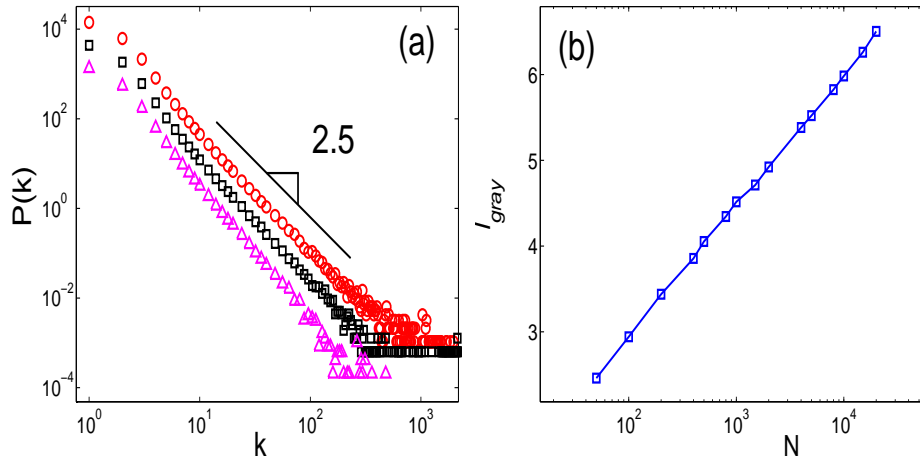
FIG. 22: (a) The degree distribution of the "gray tree" (the MST of the supernode network, shown in Fig. 20(d)), in which the supernodes are percolation clusters and the links are the gray links. Different symbols represent different threshold values: p_c ($\bigcirc$), $p_c + 0.01$ ($\square$) and $p_c + 0.02$ ($\triangle$). The distribution exhibits a scale-free tail with $\lambda \approx 2.5$, and is relatively insensitive to changes in p_c. (b) The average path length ℓ_{gray} on a the gray tree as a function of original network size. It is seen that $\ell_{\text{gray}} \sim \log N_{\text{sn}} \sim \log N$ (After [Kalisky $et.$ al, 2006]).

the supernodes. As explained above, the MST is optimal in two senses: (i) the total weight of all links is minimal (ii) any path between any two nodes on the MST will encounter the smallest maximal $barrier$ (weight) between these nodes. The last property is common to many physical systems (e.g. the protein folding network - see below). Accordingly, we study the weights encountered when traveling along a typical path on the MST.

We consider all pairs of nodes in the original MST of N nodes [Fig. 20(c)] and calculate the typical path length ℓ_{typ}, which is the most probable path length on the MST. For each path of length ℓ_{typ} we rank the weights on its links in descending order. For the largest weights ("rank 1 links"), we calculate the average weight $w_{r=1}$ over all paths. Similarly, for the next largest weights ("rank 2 links") we find the average $w_{r=2}$ over all paths, and so on up to $r = \ell_{\text{typ}}$. Fig. 23(a) shows w_r as a function of rank r for three different network sizes $N = 2000$, 8000, and 32000. It can be seen that weights below p_c (black links inside the supernodes) are uniformly distributed and approach one another as N increases. As opposed to this, weights above p_c ("gray links") are not uniformly distributed, due to the bombing algorithm, and are independent of N. Actually, weights above p_c encountered along

the optimal path (such as the largest weights w_1, w_2 and w_3) are significantly higher than those below p_c. Fig. 23(b) shows that the links with the highest weights on the MST can be associated with gray links from very small clusters [Figs. 20(a) and 20(c)] (similar results have been obtained along the optimal path).

As mentioned earlier, this property is present also in the original supernode network and hence the change in the threshold used to obtain the supernodes does not destroy the power law degree distribution but only introduces an exponential cutoff. We thereby obtain a scale-free supernode network with $\lambda = 2.5$, which is not very sensitive to the precise value of the threshold used for defining the supernodes. For example, the scale-free degree distribution shown in Fig. 22(a) for a threshold of $p_c+0.01$ corresponds to having only four largest weights on the optimal paths [see Fig. 23(a)]. However, even for $p_c + 0.02$ the degree distribution is well approximated by a scale-free distribution with $\lambda = 2.5$ [see Fig. 22(a)]. This means that mainly very small clusters, connected with high-weight links to large clusters, dominate the scale-free distribution $P(k)$ of the MST of the supernode network (gray tree). Hence, the bombing optimization process on an ER graph causes a significant separation between links below and above p_c to emerge *spontaneously* in the system, and by merging nodes connected with links of low weights, a scale-free network can arise.

The process described above may be related to the evolution of some real world networks. Consider a homogeneous network with many components whose average degree $\langle k \rangle$ is well defined. Suppose that the links between the components have different weights, and that some optimization process separates the network into nodes which are well connected (i.e., connected by links with low weights) and nodes connected by links having much higher weights. If the well-connected components merge into a single node, this results in a new heterogeneous supernode network with scale free degree distribution.

An example of a real world network whose evolution may be related to this model is the protein folding network, which was found to be scale-free with $\lambda \approx 2.3$ [Rao, 2004]. The nodes are the possible physical configurations of the system and the links between them describe the possible transitions between the different configurations. We assume that this network is *optimal* because the system chooses the path with the smallest energy *barrier* from all possible trajectories in phase space. It is possible that the scale-free distribution evolves through a similar procedure as described above for random graphs: adjacent configurations with close energies (nodes in the same cluster) cannot be distinguished and are regarded as
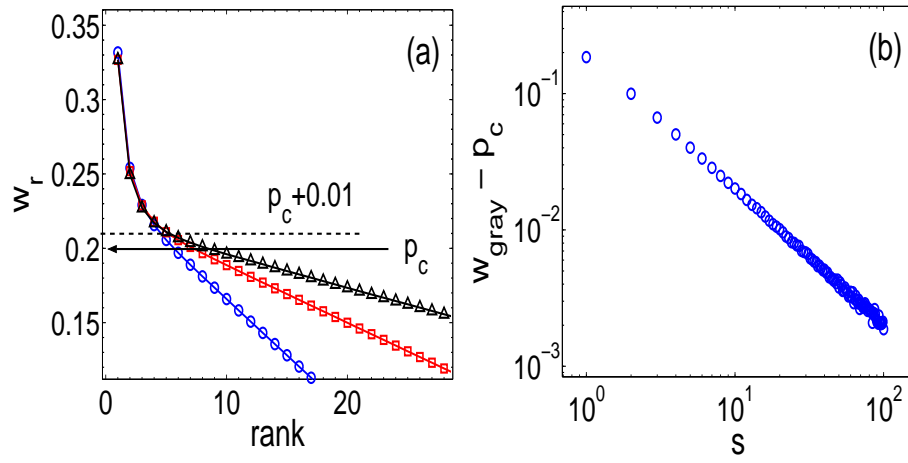
55

FIG. 23: (a) The average weights w_r along the optimal path of an ER graph with $\langle k \rangle = 5$, sorted according to their rank. Different symbols represent different system sizes: $N = 2000$ ($\bigcirc$), $N = 8000$ ($\square$) and $N = 32000$ ($\triangle$). Below $p_c = 0.2$, the weights are uniformly distributed, while weights above p_c are significantly higher and independent of N. (b) Cluster size vs. the minimal gray link emerging from each cluster, for ER graphs with $\langle k \rangle = 5$ and $N = 10000$. Small clusters are associated with higher weights because they have a small number of exits and thus cannot be optimized (After [Kalisky *et. al*, 2006]).

a single supernode, while configurations (clusters) with high barriers between them belong to different supernodes.

A second example is computer networks. Strongly interacting computers (such as computers belonging to researchers from the same company or research institution) are likely to converge into a single domain, and thus domains with various sizes and connectivities are formed. This network might be also optimal, because packets destined to an external domain are presumably routed through the router which has the best connection to the target domain.

To summarize, we have seen that any weighted random network hides an inherent scale-free "supernode network."[10] We showed that the minimum spanning tree, generated by the bombing algorithm, is composed of percolation clusters connected by a scale-free tree of "gray" links. Most of the gray links connect small clusters to large ones, thus having weights well above the percolation threshold that do not change with the original size of the network. Thus the optimization in the process of building the MST distinguishes between

links with weights below and above the threshold, leading to a spontaneous emergence of a scale-free "supernode network". We raise the possibility that in some naturally optimal real-world networks, nodes connected well merge into one single node, and thus a scale-free network emerges.

IX. PARTITION OF THE MINIMUM SPANNING TREE INTO SUPERHIGH-WAYS AND ROADS

The centrality, C, quantifies the "importance" of a node for transport in the network. Moreover, identifying the nodes with high C enables, as shown below, to improve their transport capacity and thus improve the global transport in the network. Several definitions of centrality exists. Here we deal with the "betweeness centrality" which is defined as the relative number of shortest path in the network passing through a node (or a link). The probability density function (pdf) of C was studied on the MST for both scale-free (SF) [Barabási & Albert, 1999] and Erdős-Rényi (ER) [Erdős & Rényi, 1959; Erdős & Rényi, 1960] networks and found to satisfy a power law,

$$\mathcal{P}_{\mathrm{MST}}(C) \sim C^{-\delta_{\mathrm{MST}}} \tag{77}$$

with δ_{MST} close to 2 [Goh *et al.*, 2005; Kim *et al.*, 2004]. An important question is weather there are substructure of the MST which are more central and play a major role on the transport. Reference [Wu *et al.*, 2006] shows that a sub-network of the MST, the infinite incipient percolation cluster (IIC) has a significantly higher average C than the entire MST—i.e., the set of nodes inside the IIC are typically used by transport paths more often than other nodes in the MST [Wu *et al.*, 2006]. — In this sense the IIC can be viewed as a set of *superhighways* (SHW) in the MST. The nodes on the MST which are not in the IIC are called *roads*, due to their analogy with roads of less traffic (usually used by local residents). We demonstrate the impact of this finding by showing that improving the capacity of the superhighways (IIC) is significantly a better strategy to enhance global transport compared to improving the same number of links with the highest C in the MST, although they have higher C [Wu *et al.*, 2006]. This counterintuitive result shows the advantage of identifying the IIC subsystem, which is very small compared to the full network. These results are based on extensive numerical studies for centrality of the IIC, and comparison with the

centrality of the entire MST [Wu *et al.*, 2006; Newman, 2001], as described below. ER and SF network of size N are generated by the methods explained in section II A. Multiple connections between two nodes and self-loops in a single node are disallowed. To construct a *weighted* network, a weight w_i is assigned to each link from a uniform distribution between 0 and 1. The MST is obtained from the weighted network using Prim's algorithm [Ahuja *et al.*, 1993] (see Section II E). Once the MST is built, one can compute the value of C of each node by counting the number of paths between all possible pairs passing through that node and normalize C by the total number of pairs in the MST, $N(N-1)/2$, which ensures that C is between 0 and 1.[11] The IIC of ER and SF networks is simulated as explained in Section II F.

To quantitatively study the centrality of the nodes in the IIC, we calculate the pdf, $\mathcal{P}_{\mathrm{IIC}}(C)$ of C. Figure 24 shows that for all three cases studied, ER, SF and square lattice networks, $\mathcal{P}_{\mathrm{IIC}}(C)$ for nodes satisfies a power law

$$\mathcal{P}_{\mathrm{IIC}}(C) \sim C^{-\delta_{\mathrm{IIC}}}, \tag{78}$$

where

$$\delta_{\mathrm{IIC}} \approx \begin{cases} 1.2 & [\mathrm{ER, SF}] \\ 1.25 & [\mathrm{square\ lattice}] \end{cases}. \tag{79}$$

Moreover, from Fig. 24, it is seen that $\delta_{\mathrm{IIC}} < \delta_{\mathrm{MST}}$, implying a larger probability to find a larger value of C in the IIC compared to the entire MST. The values for δ_{MST} are consistent with those found in Ref. [Goh *et al.*, 2005]. Similar results for the centrality of the links were obtained. The results thus show that the IIC is like a network of *superhighways* inside the MST. When we analyze centrality of the entire MST, the effect of the high C of the IIC is not seen since the IIC is only a tiny fraction of the MST. Some results are summarized in Table II.

The values of δ_{MST} and δ_{IIC} can be understood from the following scaling arguments, based self-similarity properties of the MST and the IIC. Similar arguments are used in [Stauffer & Aharony, 1994; Bunde & Havlin, 1996] to express exponent τ_s describing the cluster size distribution at percolation threshold on a lattice in terms of the cluster fractal dimension and the dimension of the lattice. Indeed, the majority of nodes are connected through the superhighway links, whose centrality is proportional to N^2. The number of these links for the entire network scales as $\ell_\infty(N) \sim N^{1/\nu_{opt}}$ [Braunstein *et al.*, 2003; Wu *et*

al., 2005]. Thus small regions of the MST of chemical diameter ℓ consists of $n^{1/\nu_{\text{opt}}}$ nodes. These regions have length $\ell_\infty(n) \sim n^{1/\nu_{\text{opt}}}$. These roads connect the nodes in this region with the rest of the nodes of the MST, and thus their centrality is at least nN. The total number of such links in all the regions of size n is $m(n) = \ell_\infty(n)N/n \sim n^{\nu_{\text{opt}}-1}$. This is the number of links with centrality larger than nN. Thus number of links with centrality exactly nN is $m(n) - m(n+1) \sim n^{\nu_{\text{opt}}-2} = n^{-\delta_{\text{MST}}}$. Using Eq. (38) we have:

$$
\delta_{\text{MST}} = \begin{cases} 5/3, \ \lambda > 4, \quad \text{ER} \\ (\lambda+1)/(\lambda-1), \ 3 < \lambda \leq 4 \end{cases} .
\tag{80}
$$

Similar arguments lead to the centrality distribution of the nodes on the IIC. The small regions of chemical diameter ℓ have centrality larger or equal to $Nn(\ell)$. The number of links in the IIC belonging to these regions is $s(\ell) = \ell^{d_\ell}$ [Cohen $et\ al.$, 2002]. The total number of such regions is $S/s(\ell)$, thus the total number of the links of the IIC with centrality larger than $Nn(\ell)$ is $m[n(\ell)] = \ell/s(\ell) \sim \ell^{1-d_\ell} = n^{(1-d_\ell)\,\nu_{\text{opt}}}$. Accordingly

$$
\delta_{\text{IIC}} = 1 + (d_\ell - 1)\nu_{\text{opt}} = \begin{cases} 4/3, \ \lambda > 4, \quad \text{ER} \\ \lambda/(\lambda-1), \ 3 < \lambda \leq 4 \end{cases} .
\tag{81}
$$

The values predicted by Eqs. (80) and (81) are in good agreement with the simulation results presented in Table II.

To further demonstrate the significance of the IIC, we compute the average $\langle C \rangle$ for each realization of the network over all nodes. Fig. 27, shows the histograms of $\langle C \rangle$ for both the IIC and for the other nodes on the MST. We see that the nodes on the IIC have significantly larger $\langle C \rangle$ compared to the other nodes of the MST.

	ER	SF ($\lambda = 4.5$)	SF ($\lambda = 3.5$)	square lattice
δ_{IIC}	1.2	1.2	1.2	1.25
δ_{MST}	1.6	1.7	1.7	1.32
ν_{opt}	1/3	1/3	0.2	0.61
$\langle u \rangle$	0.29	0.20	0.13	0.64

TABLE II: Results for the IIC and the MST (After [Wu $et\ al.$, 2006]).

Figure 25 shows a schematic plot of the SHW inside the MST and demonstrates its use by the path between pairs of nodes. The MST is a "skeleton" subset of links inside the
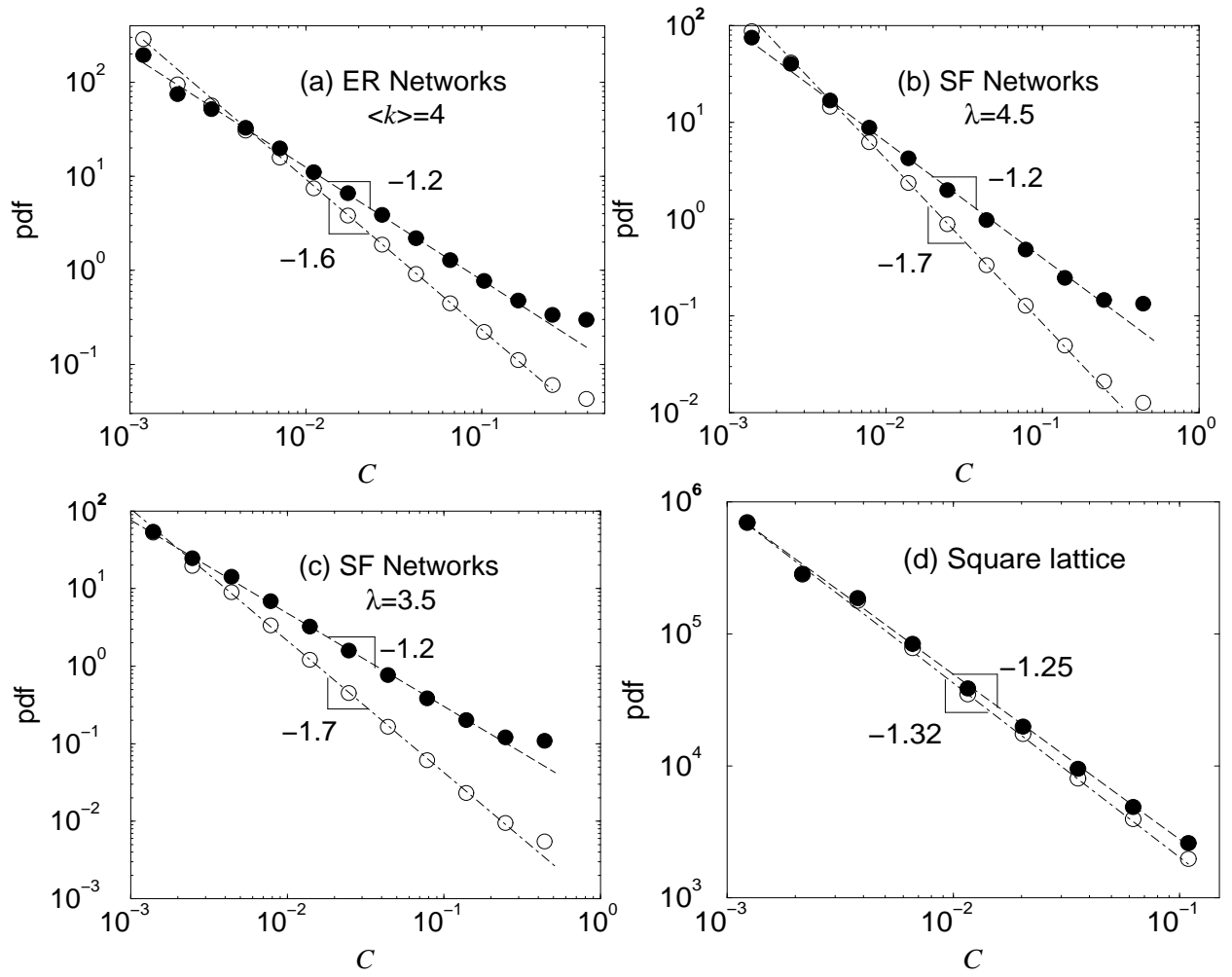
FIG. 24: The pdf of the centrality C of nodes for (a) ER graph with $\langle k \rangle = 4$, (b) SF with $\lambda = 4.5$, (c) SF with $\lambda = 3.5$ and (d) 90×90 square lattice. For ER and SF, $N = 8192$ and for the square lattice $N = 8100$. We analyze 10^4 realizations. For each graph, the full circles show $\mathcal{P}_{\mathrm{IIC}}(C)$; the empty circles show $\mathcal{P}_{\mathrm{MST}}(C)$ (After [Wu *et al.*, 2006]).

network, which plays a key role in transport between the nodes. However, the IIC in the MST is like the "spine in the skeleton", which plays the role of the superhighways inside a road transportation system. To illustrate our result a car can drive from the entry node A on roads until it reaches a superhighway, and finds the exit which is closest to node B. Thus those nodes which are far from each other in the MST use the IIC superhighways more than those nodes which are close to each other. In order to demonstrate this, we compute f, the average fraction of pairs of nodes using by the shortest paths the IIC, as a function of ℓ_{MST}, the distance between a pair of nodes on the MST (Fig. 26). We see that f increases and
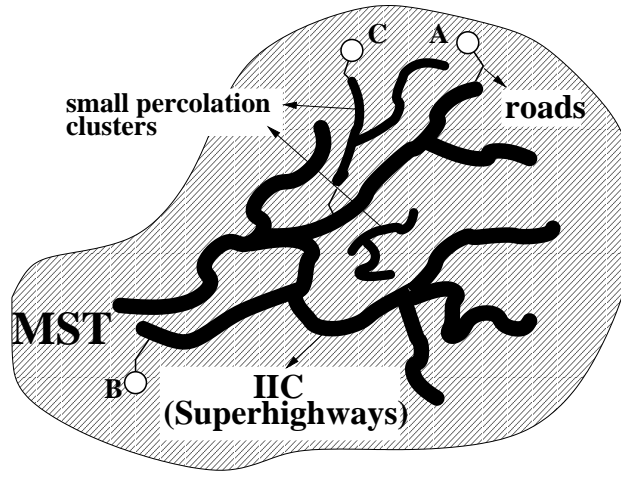
FIG. 25: Schematic graph of the network of connected superhighways (heavy lines) inside the MST (shaded). A, B and C are examples of possible entry and exit nodes, which connect to the network of superhighways by "roads" (thin lines). The middle size lines indicate other percolation clusters with much smaller size compared to the IIC (After [Wu *et al.*, 2006]).

approaches one as ℓ_{MST} grows. We also show that f scales as $\ell_{\mathrm{MST}}/N^{\nu_{\mathrm{opt}}}$ for different system sizes, where ν_{opt} is the percolation connectedness exponent [Braunstein *et al.*, 2003; Wu *et al.*, 2005].

The next question is how much the IIC is used in transport on the MST? We define the *IIC superhighway usage*,

$$u \equiv \frac{\ell_{\mathrm{IIC}}}{\ell_{\mathrm{MST}}}, \tag{82}$$

where ℓ_{IIC} is the number of links in a given path of length ℓ_{MST} belonging to the IIC superhighways. The average usage $\langle u \rangle$ quantifies what fraction of nodes/links of the IIC is used by the transport between all pairs of nodes. In Fig. 28(a), we show $\langle u \rangle$ as a function of the system size N. Our results suggest that $\langle u \rangle$ approaches a constant value and becomes independent of N for large N. This is surprising since the average value of the ratio between the number of nodes on the IIC and on the MST, $\langle N_{\mathrm{IIC}}/N_{\mathrm{MST}} \rangle$, approaches zero as $N \to \infty$, showing that although the IIC contains only a tiny fraction of the nodes in the entire network, its usage for the transport in the entire network is constant. We find that $\langle u \rangle \approx 0.3$ for ER networks, $\langle u \rangle \approx 0.2$ for SF networks with $\lambda = 4.5$, and $\langle u \rangle \approx 0.64$ for the square lattice. The reason why $\langle u \rangle$ is not close to 1.0 is that in addition to the IIC, the optimal path passes also through other percolation clusters, such as the second largest and the third largest
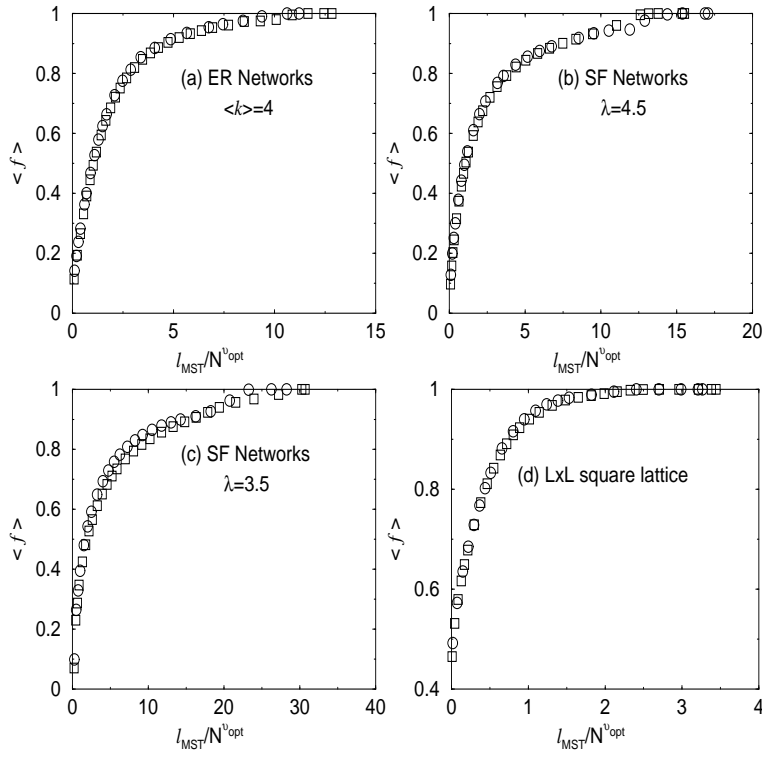
61

FIG. 26: The average fraction, $\langle f \rangle$, of pairs using the SHW, as a function of ℓ_{MST}, the distance between the pair on the MST. (a) ER graph with $\langle k \rangle = 4$, (b) SF with $\lambda = 4.5$, (c) SF with $\lambda = 3.5$ and (d) square lattice. For ER and SF: ($\bigcirc$)$N = 1024$ and ($\square$)$N = 2048$ with 10^4 realizations. For square lattice: ($\bigcirc$)$N = 1024$ and ($\square$)$N = 2500$ with 10^3 realizations. The x axis is rescaled by $N^{\nu_{\mathrm{opt}}}$, where $\nu_{\mathrm{opt}} = 1/3$ for ER and for SF with $\lambda > 4$, and $\nu_{\mathrm{opt}} = (\lambda - 3)/\lambda - 1)$ for SF networks with $3 < \lambda < 4$ [Braunstein *et al.*, 2003]. For the $L \times L$ square lattice, $\ell_{\mathrm{MST}} \sim L^{d_{\mathrm{opt}}}$ with $d_{\mathrm{opt}} = 1.22$ and since $L^2 = N$, $\nu_{\mathrm{opt}} = d_{\mathrm{opt}}/2 \approx 0.61$ [Cieplak *et al.*, 1996; Porto *et al.*, 1999] (After [Wu *et al.*, 2006]).

percolation clusters. In Fig. 28, we also show for ER networks, the average usage of the two largest and the three largest percolation clusters for a path on the MST and we see that the average usage increases significantly and is also independent of N. However, the number of clusters used by a path on MST is relatively small and proportional to $\ln N$ [Sreenivasan *et al.*, 2004], suggesting that the path on the MST uses only few percolation clusters and few jumps between them (of order $\ln N$) when traveling from an entry node to an exit node on the network. When $N \to \infty$ the average usage of all percolation clusters should approach 1.

Can we use the above results to improve the transport in networks? It is clear that by
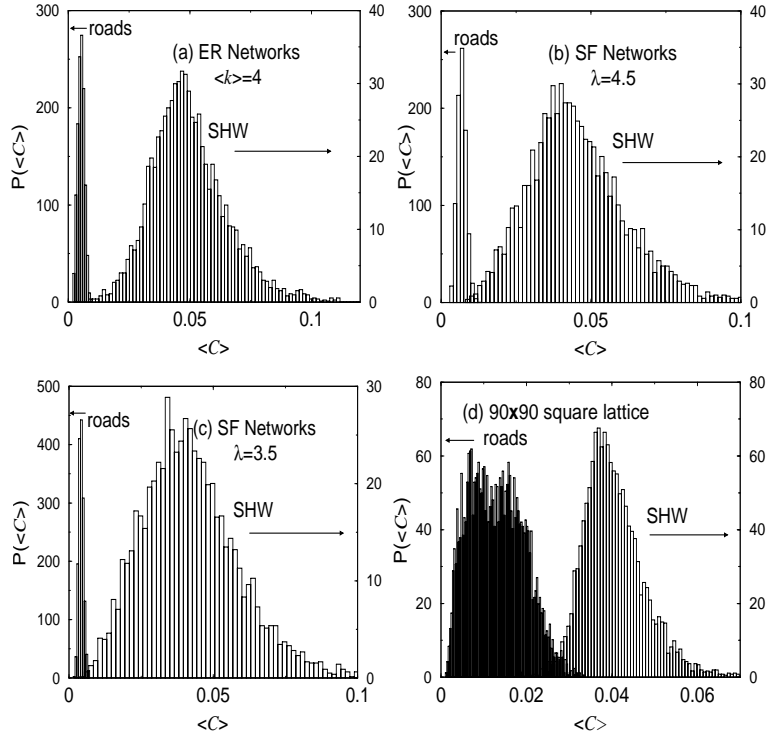
FIG. 27: The normalized pdf for superhighway and roads of $\langle C \rangle$, the C averaged over all nodes in one realization. (a) ER network, (b) SF network with $\lambda = 4.5$, (c) SF network with $\lambda = 3.5$ and (d) square lattice network. To make each histogram, we analyze 1000 network configurations (After [Wu *et al.*, 2006]).

improving the capacity or conductivity of the highest C links one can improve the transport (see Fig. 28(b) inset). We hypothesize that improving the IIC links (strategy I), which represent the superhighways is more effective than improving the same number of links with the highest C in the MST (strategy II), although have higher centrality. To test the hypothesis, we study two transport problems: (i) current flow in random resistor networks, where each link of the network represents a resistor and (ii) the maximum flow problem well known in computer science [Cormen *et al.*, 1990]. We assign to each link of the network a resistance/capacity, e^{ax}, where x is an uniform random number between 0 and 1, with $a = 40$. The value of a is chosen such as to have a broad distribution of disorder so that the MST carries most of the flow [Wu *et al.*, 2005; Sreenivasan *et al.*, 2004]. We randomly choose n pairs of nodes as sources and other n nodes as sinks and compute the flow between them. We compare the transport by improving the conductance/capacity of all links on the
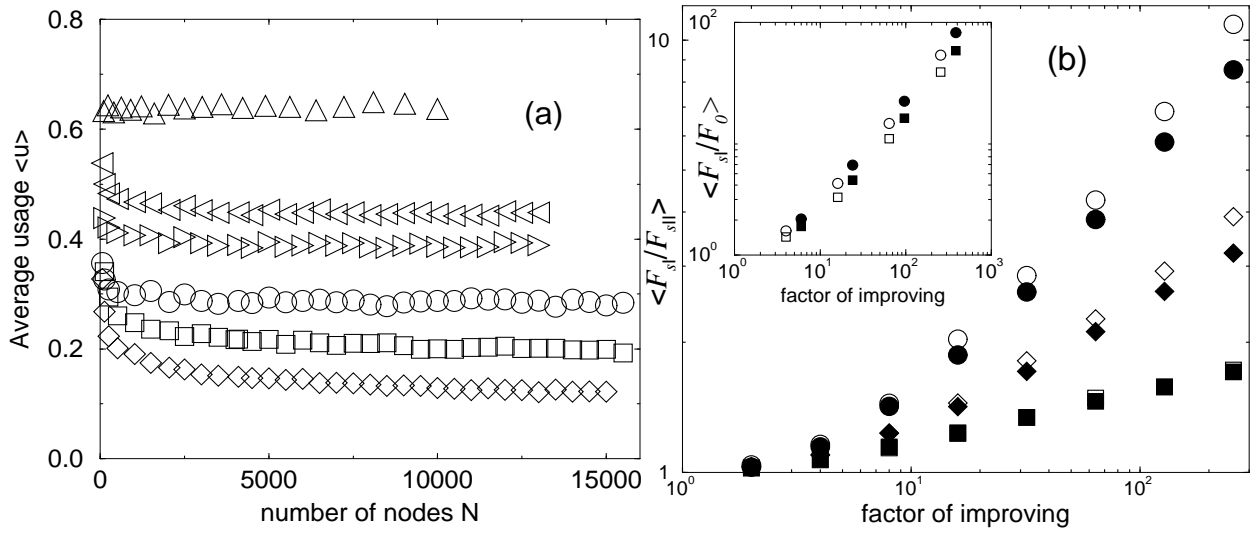
FIG. 28: (a) The average usage $\langle u \rangle \equiv \langle \ell_{\mathrm{IIC}}/\ell_{\mathrm{MST}} \rangle$ for different networks, as a function of the number of nodes N. $\bigcirc$ (ER with $\langle k \rangle = 4$), $\square$ (SF with $\lambda = 4.5$), $\Diamond$ (SF with $\lambda = 3.5$), $\triangle$ ($L \times L$ square lattice). The symbols ($\triangleright$) and ($\triangleleft$) represent the average usage for ER with $\langle k \rangle = 4$ when the two largest percolation clusters and the three largest percolation clusters are taken into account, respectively. (b) The ratio between the flow using strategy I, $F_{s\mathrm{I}}$, and that using strategy II, $F_{s\mathrm{II}}$, as a function of the factor of improving conductivity/capacity. The inset is the ratio between the flow using strategy I and the flow in the original network, F_0. The data are all for ER networks with $N = 2048$, $\langle k \rangle = 4$ and $n = 50(\bigcirc)$, $n = 250(\Diamond)$ and $n = 500(\square)$. The unfilled symbols are for current flow and the filled symbols are for maximum flow (After [Wu $et\ al.$, 2006]).

IIC (strategy I) with that by improving the same number of links with the highest C in the MST (strategy II). Since the two sets are not the same and therefore higher centrality links will be improved in II, it is tempting to suggest that the better strategy to improve the global flow is strategy II. However, here we demonstrate using ER networks as an example that counterintuitively strategy I is better. We also find similar advantage of strategy I compared to strategy II for SF networks with $\lambda = 3.5$.

In Fig. 28(b), we compute the ratio between the flow using strategy I ($F_{s\mathrm{I}}$) and the flow using strategy II ($F_{s\mathrm{II}}$) as a function of the factor of improving conductivity/capacity of the links. The figure clearly shows that strategy I is better than strategy II. Since the number of links in the IIC is relatively very small comparing to the number of links in the whole network, it could proven to be a very efficient strategy.

64

In summary, we find that the centrality of the IIC for transport in networks is significantly larger than the centrality of the other nodes in the MST. Thus the IIC is a key component for transport in the MST. We demonstrate that improving the capacity/conductance of the links in the IIC is useful strategy to improve transport.

X.   SUMMARY

We reviewed recent studies on the scaling of the average optimal path length ℓ_{opt} in a disordered network. There are two scaling regimes of ℓ_{opt} corresponding to the regimes of weak and strong disorder. For ER networks and SF networks with $\lambda > 4$, $\ell_{\mathrm{opt}} \sim \ln N$ in the weak disorder regime while $\ell_{\mathrm{opt}} \sim N^{1/3}$ in the strong disorder regime. For SF networks with $3 < \lambda < 4$, $\ell_{\mathrm{opt}} \sim \ln N$ in the weak disorder regime while $\ell_{\mathrm{opt}} \sim N^{\frac{\lambda-3}{\lambda-1}}$ in the strong disorder regime. For SF networks with $2 < \lambda < 3$, $\ell_{\mathrm{opt}} \sim \ln N$ in the weak disorder regime while $\ell_{\mathrm{opt}} \sim \ln^{\lambda-1} N$ in the strong disorder regime. The scaling behavior of ℓ_{opt} in the strong disorder regime for ER and SF networks with $\lambda > 3$ is obtained analytically using percolation theory.[12] For exponential disorder, for both ER random networks and SF networks we obtain a scaling function for the crossover from weak disorder characteristics to strong disorder characteristics. We show that the crossover occurs when the min-max path reaches a crossover length $\ell^*(a)$ and $\ell^*(a) \sim a$. Equivalently, the crossover occurs when the network size N reaches a crossover size $N^*(a)$, where $N^*(a) \sim a^3$ for ER networks and for SF networks with $\lambda \geq 4$ and $N^*(a) \sim a^{\frac{\lambda-1}{\lambda-3}}$ for SF networks with $3 < \lambda < 4$.

We also have shown that the optimal path length distribution in weighted random graphs has a universal scaling form according to Eq. (76). We explain this behavior and demonstrate the transition between polynomial to logarithmic behavior of the average optimal path in a single graph.

Our results are consistent with results found for finite dimensional systems [Porto et $al.$, 1999; Wu et $al.$, 2005; Strelniker $et.$ al, 2005; Perlsman & Havlin, 2005]: In finite dimension the parameter controlling the transition is $\frac{L^{1/\nu}}{ap_c}$, where L is the system length and ν is the correlation length critical exponent. This is because only the "red bonds" - bonds that if cut would disconnect the percolation cluster [Stanley, 1977, Coniglio, 1982] - control the transition.

We also show that any weighted random network hides an inherent scale-free "supernode

network." We showed that the minimum spanning tree, generated by the bombing algorithm, is composed of percolation clusters connected by a scale-free tree of "gray" links. Most of the gray links connect small clusters to large ones, thus having weights well above the percolation threshold that do not change with the size of the network. Thus the optimization in the process of building the MST distinguishes between links with weights below and above the threshold, leading to a spontaneous emergence of a scale-free "supernode network" with $\lambda = 2.5$. We raise the possibility that in some naturally optimal real-world networks, nodes connected well merge into one single node, and thus a scale-free network emerges.

The centrality in networks for transport on the MST is studied. We found that the centrality of the nodes in the IIC is significantly larger than the centrality of the other nodes in the MST. The analytical estimation for the exponents of the centrality distribution for both the MST and the IIC are provided. Thus the IIC is a key component for transport in the MST. As a result of this finding, we demonstrated that improving the capacity/conductance of the links in the IIC is a useful strategy to improve transport which is a better strategy compare to improving the same number of links with the highest centrality in the MST. This is probably due to the global nature of transport which prefer global improvement of the superhighways rather than local improvement of high centrality links.

References

Albert, R. & Barabási, A.-L. [2002] "Statistical mechanics of complex networks," *Rev. Mod. Phys.* **74**, 47–97.

Ahuja, R. K., Magnanti, T. L. & Orlin, J. B. [1993] *Network Flows: Theory, Algorithms and Applications* (Prentice-Hall, Englewood Cliffs).

Barabási, A.-L. [1996] "Invasion Percolation and Global Optimization", Phys. Rev. Lett. **76**, 3750.

Barabási, A.-L. & Albert, R. [1999] "Emergence of Scaling in Random Networks", Science

286, 509.

Barabási, A.-L. [2002] *Linked: The New Science of Networks* (Perseus Publishing, Cambridge MA).

Barrat, A. *et al.*[2004] "The architecture of complex weighted networks", PNAS, **101**, 3747.

Barthélémy, M. & Amaral, L. A. N. [1999] "Small-World Networks: Evidence for a Crossover Picture", Phys. Rev. Lett. **82**, 3180.

Boccaletti, S., Latora, V., Moreno, Y., Chavez, M. & Hwang, D.-U. [2006] "Complex networks: Structure and dynamics", Physics Reports **424**, 175.

Bollobas, B. [1985] *Random Graphs* (Academic, London).

Bonanno, G., Caldarelli, G., Lillo, F. & Mantegna, R. N. [2003] "Topology of correlation-based minimal spanning trees in real and model markets", Phys. Rev. E **68**, 046130.

Braunstein, L. A., Buldyrev, S. V., Havlin, S. & Stanley, H. E. [2001] "Universality classes for self-avoiding walks in a strongly disordered system", Phys. Rev. E **65**, 056128.

Braunstein, L. A., Buldyrev, S. V., Cohen, R., Havlin, S. & Stanley, H. E. [2003] "Optimal paths in disordered complex networks", Phys. Rev. Lett. **91**, 168701.

Braunstein, L. A. Buldyrev, S. V., Sreenivasan, S., Cohen, R., Havlin, S. & Stanley, H. E. [2004] "The optimal path in a random network", *Lecture Notes in Physics: Proceedings of the 23rd CNLS Conference, "Complex Networks," Santa Fe 2003*, edited by E. Ben-Naim, H. Frauenfelder & Z. Toroczkai (Springer, Berlin).

Buchanan, M. [2002] *Nexus: Small Worlds and the Groundbreaking Theory of Networks* (W. W. Norton, New York).

Buldyrev, S. V., Braunstein, L. A., Cohen, R., Havlin, S. & Stanley, H. E. [2003] "Length of optimal path in random networks with strong disorder", Physica A **330**, 246.

Buldyrev, S. V., Havlin, S. & Stanley, H. E. [2006] "Optimal paths in strong and weak disorder: A unified approach", Phys. Rev. E **73**, 036128.

Bunde, A. & Havlin, S., eds. [1996] *Fractals and Disordered Systems* (Springer, New York).

Callaway, D. S., Newman, M. E. J., Strogatz, S. H. & Watts, D. J. [2000] "Network Robustness and Fragility: Percolation on Random Graphs", Phys. Rev. Lett., **85**, 5468–5471.

Chen, Y. *et al.* [2006] "Universal Behavior of Optimal Paths in Weighted Networks with

General Disorder", Phys. Rev. Lett. **96**, 068702.

Cieplak, M., Maritan, A. & Banavar, J. R. [1994] "Optimal paths and domain walls in the strong disorder limit", Phys. Rev. Lett. **72** 2320.

Cieplak, M., Maritan, A. & Banavar, J. R. [1996] "Invasion Percolation and Eden Growth: Geometry and Universality", Phys. Rev. Lett. **76**, 3754.

Cohen, R., Erez, K., ben-Avraham, D. & Havlin, S. [2000] "Resilience of the Internet to Random Breakdowns", Phys. Rev. Lett. **85**, 4626.

Cohen, R. ben-Avraham, D. & Havlin, S. [2002] "Percolation critical exponents in scale-free networks", Phys. Rev. E **66**, 036113.

Cohen, R. & Havlin, S. [2003] "Scale free networks are ultrasmall", *Phys. Rev. Lett.* **90**, 058701.

Cohen, R., Havlin, S. & ben-Avraham, D. [2002] "Structural properties of scale free networks", in *Handbook of Graphs and Networks*, edited by S. Bornholdt and H. G. Shuster (Willey-VCH, New York), Ch. 4.

Coniglio, A. [1982] "Cluster structure near the percolation threshold", J. Phys. A. **15**, 3829–3844.

Cormen, T. H., Leiserson, C. E. & Rivest, R. L. [1990] *Introduction to Algorithms* (MIT Press, Cambridge MA).

de Gennes, P.-G. [1979] *Scaling Concepts in Polymer Physics* (Cornell University Press, Ithaca).

Dobrin, R. & Duxbury, P. M. [2001] "Minimum Spanning Trees on Random Networks", Phys. Rev. Lett. **86**, 5076.

Dorogovtsev, S. N. & Mendes, J. F. F. [2003] *Evolution of Networks: From Biological Nets to the Internet and WWW* (Oxford University Press, Oxford).

Erdős, P. & Rényi, A. [1959] "On random graphs", *Publicationes Mathematicae* **6**, 290.

Erdős, P. & Rényi, A. [1960] "On the evolution of random graphs" *Publications of the Mathematical Inst. of the Hungarian Acad. of Sciences* **5**, 17.

Fredman, M. L. & Tarjan, R. E. [1987] "Fibonacci heaps and their uses in improved network optimization algorithms", J. ACM **34**, 596.

Grassberger, P. & Zhang, Y. C. [1996] "Self-organized formulation of standard percolation phenomena", Physica A **224**, 169.

Goh, K.-I., Kahng, B. & Kim, D. [2001] "Universal Behavior of Load Distribution in

Scale-Free Networks", Phys. Rev. Lett. **87**, 278701.

Goh, K.-I., Noh, J. D. Kahng, B. & Kim, D. [2005] "Load distribution in weighted complex networks", Phys. Rev. E **72**, 017102.

Hansen, A. & Kertész, J. [2004] "Phase Diagram of Optimal Paths", Phys. Rev. Lett. **93**, 040601.

Harris, T. E. [1989] *The Theory of Branching Processes* (Dover Publication Inc., New York).

Havlin, S., Braunstein, L. A., Buldyrev, S. V., Cohen, R., Kalisky, T., Sreenivasan, S. & Stanley, H. E. [2005] "Optimal paths in Random Networks with Disorder: A Mini Review," Physica A **346**, 82–92.

Ioselevich, A. S. & Lyubshin, D. S. [2004] "Phase transition in a self-repairing random network", JETP Lett. **79**, 231.

Kalisky, T., Braunstein, L. A., Buldyrev, S. V., Havlin, S. & Stanley, H. E. [2005] "Scaling of optimal-path-lengths distribution in complex networks", Phys. Rev. E **72**, 025102(R).

Kalisky, T., Sreenivasan, S., Braunstein, L. A., Havlin, S. & Stanley, H. E. [2006] "Scale-free networks emerging from weighted random graphs", Phys. Rev. E **73**, 025103(R).

Kalisky, T. & Cohen, R. [2006] "Width of Percolation Transition in Complex Networks", Phys. Rev. E **73**, 035101.

Khan, M., Pandurangan, G. & Bhargava, B. [2003] "Energy-Efficient Routing Schemes for Sensor Networks", Tech. Rep. CSD TR 03-013, Dept. of Computer Science, Purdue University.

Kim, D.-H., Noh, J. D. & Jeong, H. [2004] "Scale-free trees: The skeletons of complex networks", Phys. Rev. E **70**, 046126.

Kruskal, J. B. [1956] "On the shortest spanning subtree and the traveling salesman problem", Proc. Amer. Math. Soc. **7**, 48.

Macdonald, P. J., Almaas, E. & Barabási, A.-L. [2005] "Minimum spanning trees of weighted scale-free networks", Europhys. Lett. **72** (2), 308.

Mendes, J. F. F., Dorogovtsev, S. N., & Ioffe, A. F. [2003] *Evolution of Networks: From Biological Nets to the Internet and the WWW* (Oxford University Press, Oxford).

Molloy, M. & Reed, B. [1995] "A critical-point for random graphs with a given degree sequence", Random Structures and Algorithms **6**, 161.

Molloy, M. & Reed, B. [1998] "The size of the giant component of a random graph with

a given degree sequence ", Combin. Probab. Comput. **7**, 295.

Newman, M. E. J. [2001] "Scientific collaboration networks. I. Network construction and fundamental results", Phys. Rev. E **64**, 016131.

Newman, M. E. J. [2001] "Scientific collaboration networks. II. Shortest paths, weighted networks, and centrality", Phys. Rev. E **64**, 016132.

Onnela, J.-P. *et al.* [2003] "Dynamics of market correlations: Taxonomy and portfolio analysis", Phys. Rev. E **68**, 056110.

Pastor-Satorras, R. & Vespignani, A. [2004] *Structure and Evolution of the Internet: A Statistical Physics Approach* (Cambridge University Press, Cambridge).

Perlsman, E. & Havlin, S. [2005] "Directed polymer - directed percolation transition: the strong disorder case", Eur. Phys. J. B **43**, 517.

Perlsman, E. & Havlin, S. [2006] "Optimal paths as correlated random walks", Europhys. Lett. **73**, 178.

Porto, M., Havlin, S., Schwarzer, S. & Bunde, A. [1997] "Optimal Path in Strong Disorder and Shortest Path in Invasion Percolation with Trapping", Phys. Rev. Lett. **79**, 4060.

Porto, M., Schwartz, N., Havlin, S. & Bunde, A. [1999] "Optimal paths in disordered media: Scaling of the crossover from self-similar to self-affine behavior", Phys. Rev. E **60**, 2448(R).

Rao, A. & Caflisch, F. [2004] "The protein folding network", J. Mol. Biol. **342**, 299.

Skiena, S. [1990] *Implementing Discrete Mathematics: Combinatorics and Graph Theory With Mathematica* (Addison-Wesley, NY).

Smailer, I., Machta, J. & Redner, S. [1993] "Exact enumeration of self-avoiding walks on lattices with random site energies", Phys. Rev. E **47**, 262.

Sreenivasan, S., Kalisky, T., Braunstein, L. A., Buldyrev, S. V., Havlin, S. & Stanley, H. E. [2004] "Effect of disorder strength on optimal paths in complex networks", Phys. Rev. E **70**, 046133.

Sreenivasan, S., Kalisky, T., Braunstein, L. A., Buldyrev, S. V., Havlin, S. & Stanley, H. E. [2005] "Transition between Strong and Weak Disorder Regimes on the Optimal Path," Physica A **346**, 174–182.

Stanley, H. E. [1977] "Cluster Shapes at the Percolation Threshold: An Effective Cluster Dimensionality and its Connection with Critical-Point Exponents", Journal of Physics A **10**, L211–L220.

Stauffer, D. & Aharony, A. [1994] *Introduction to Percolation Theory* (Taylor & Francis, London).

Strelniker, Y. M. *et al.* [2004] "Percolation transition in a two-dimensional system of Ni granular ferromagnets", Phys. Rev. E **69**, 065105(R).

Strelniker, Y. M., Havlin, S., Berkovits, R. & Frydman, A. [2005] "Resistance distribution in the hopping percolation model", Phys. Rev. E **72**, 016121.

Szabó, G. J., Alava, M. & Kertész, J. [2003] "Geometry of minimum spanning trees on scale-free networks", Physica A **330**, 31 (2003).

van der Hofstad, R., Hooghienstra, G. & van Mieghem, P. [2001] " First passage percolation on the random graph", Prob. Eng. Inf. Sciences **15**, 225.

Watts, D. J. [2003] *Six Degrees: The Science of a Connected Age* (W. W. Norton, New York).

Wu, Z. *et al.* [2005] "Current flow in random resistor networks: The role of percolation in weak and strong disorder", Phys. Rev. E **71**, 045101(R).

Wu, Z., Braunstein, L. A., Havlin, S. & Stanley, H. E. [2006] "Minimum Spannig Tree: Highways and Small Roads," Phys. Rev. Lett. **96**, 148702.

---

[1] The IIC contains loops in lattices in dimension d below 6. However, for networks ($d = \infty$), in the IIC loops can be neglegted and in this case for large N and therefore the IIC must be a subset of the MST. In our simulations, we found that more than 99% links of IIC belong to MST. For lattices, we only choose the part of the IIC that belongs to the MST.

[2] The overlap between the two groups is about 30% for ER networks of size $N = 8192$

[3] The ratio $\langle N_{\text{IIC}}/N_{\text{MST}} \rangle$ approaches zero for large $N_{\text{MST}} \equiv N$ due to the fractal nature of the IIC. Indeed, $N_{\text{IIC}} \sim N^{2/3}$ both for ER [Erdős & Rényi, 1959] and for SF with $\lambda > 4$ [Cohen]. For SF with $\lambda = 3.5$, $N_{\text{IIC}} \sim N^{0.6}$ [Cohen] and for the $L \times L$ square lattice $N_{\text{IIC}} \sim L^{91/48} \sim N^{91/96}$ [Bunde & Havlin, 1996].

[4] By uncorrelated we mean that the weights are not correlated with the topology, such as the degree of nodes.

[5] The maximal random number, is the first random number in the bombing process that we cannot remove without breaking the connection between a pair of nodes. In other words it

is the value that dominate the sum of the costs in the SD limit (see Ref. [Braunstein *et al.*, 2003; Braunstein *et al.*, 2004]).

[6] This is a consequence of the fact that for the original network the clusters at percolation have sizes s distributed as $P(s) \sim s^{-\tau}$ [Cohen *et al.*, 2002], (with $\tau = 2.5$ for ER networks and for SF networks with $\lambda \geq 4$, and $\tau = (2\lambda - 3)/(\lambda - 2)$ for SF networks with $3 < \lambda < 4$) and each node within this cluster has a non-zero probability of connecting to a node outside the cluster.

[7] Note that the minimal degree is $m = 2$ thus ensuring that there exists an infinite cluster for any λ, and thus $0 < p_c < 1$. For the case of $m = 1$ there is almost surely no infinite cluster for $\lambda > \lambda_c \approx 4$ (or for a slightly different model, $\lambda_c = 3.47875$), resulting in an effective percolation threshold $p_c = \frac{\langle k \rangle}{\langle k(k-1) \rangle} > 1$.

[8] MSTs on scale-free networks were found to retain the original network's degree distribution [Szabó *et al.*, 2003; Kim *et al.*, 2004; Macdonald *et al.*, 2005].

[9] MSTs on scale-free networks with $\lambda = 2.5$ were found to retain the original network's degree distribution.

[10] Similar results can also be obtained for graphs embedded in two or three dimensions, with different power law exponents.

[11] This C measurement is equivalent to counting the number of times a node (link) is used by the set of optimal paths linking all pairs of nodes, in the limit of strong disorder.

[12] The results for SF networks with $2 < \lambda < 3$ have been obtained numerically and a theoretical explanation for these results is still pending.